BIOCHEMISTRY
including biophysical chemistry & molecular biology

Article

pubs.acs.org/biochemistry

Specificity of Lipoprotein-Associated Phospholipase A_2 toward Oxidized Phosphatidylserines: Liquid Chromatography–Electrospray Ionization Mass Spectrometry Characterization of Products and Computer Modeling of Interactions

Vladimir A. Tyurin,*[,†,‡] Naveena Yanamala,[†,§] Yulia Y. Tyurina,[†,‡] Judith Klein-Seetharaman,[§] Colin H. Macphee,[∥] and Valerian E. Kagan*[,†,‡]

[†]Center for Free Radical and Antioxidant Health, [‡]Department of Environmental and Occupational Health, and [§]Department of Structural Biology, University of Pittsburgh, Pittsburgh, Pennsylvania 15260, United States

[∥]GlaxoSmithKline, King of Prussia, Pennsylvania 19406, United States

ABSTRACT: Ca^{2+}-independent lipoprotein-associated phospholipase A_2 (Lp-PLA_2) is a member of the phospholipase A_2 superfamily with a distinguishing characteristic of high specificity for oxidatively modified *sn*-2 fatty acid residues in phospholipids that has been especially well characterized for peroxidized species of phosphatidylcholines (PC). The ability of Lp-PLA_2 to hydrolyze peroxidized species of phosphatidylserine (PS), acting as a recognition signal for clearance of apoptotic cells by professional phagocytes, as well as the products of the reaction has not been investigated. We performed liquid chromatography–electrospray ionization mass spectrometry-based structural characterization of oxygenated, hydrolyzed molecular species of PS-containing linoleic acid in either the *sn*-2 position ($C_{18:0}/C_{18:2}$) or in both *sn*-1 and *sn*-2 positions ($C_{18:2}/C_{18:2}$), formed in the cytochrome *c*- and H_2O_2-driven enzymatic oxidation reaction. Cytochrome *c* has been chosen as a catalyst of peroxidation reactions because of its likely involvement in PS oxidation in apoptotic cells. We found that Lp-PLA_2 catalyzed the hydrolysis of both nontruncated and truncated (oxidatively fragmented) species of oxidized PS species, albeit with different efficiencies, and performed detailed characterization of the major reaction products: oxygenated derivatives of linoleic acid as well as nonoxygenated and oxygenated species of lyso-PS. Among linoleic acid products, derivatives oxygenated at the C_9 position, including 9-hydroxyoctadecadienoic acid (9-HODE), a potent ligand of G protein-coupled receptor G2A, were the most abundant. Computer modeling of interactions of Lp-PLA_2 with different PS-oxidized species indicated that they are able to bind in the proximity (<5 Å) of Ser273 and His351 of the catalytic triad. For 9-hydroxy and 9-hydroperoxy derivatives of oxidized PS, the *sn*-2 ester bond was positioned very close (<3 Å) to the Ser273 residue, a nucleophile directly attacking the *sn*-2 bond, thus favoring the hydrolysis reaction. We suggest that oxidatively modified free fatty acids and lyso-PS species generated by Lp-PLA_2 may represent important signals facilitating and regulating the execution of apoptotic and phagocytosis programs essential for the control of inflammation.

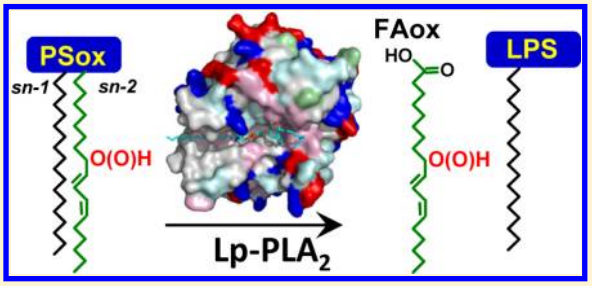

Diversity of phospholipids, including a large variety of their polyunsaturated species, is essential for the normal physiology of mammalian cells.[1,2] Most commonly, polyunsaturated acyl residues are localized in the *sn*-2 position, whereas saturated and monounsaturated fatty acids are linked at the *sn*-1 position of the glycerol backbone. However, saturated, monounsaturated, and polyunsaturated residues may be present in both *sn*-1 and *sn*-2 positions, and the abundance of these species varies depending on the type of tissue, cell, or organelle as well as on nutritional and (patho)physiological conditions.[3,4] For example, the level of polyunsaturated fatty acids esterified at the *sn*-1 position may significantly increase during phospholipid remodeling, transacylation, under low-fat diet supplementation.[5,6] The *sn* position of polyunsaturated acyl residues in the phospholipid glycerol backbone has a significant impact on the membrane function, cell signaling, and substrate specificity of various enzymes.[7]

The presence of multiple double bonds makes lipids susceptible to catalytic oxidative modifications, with the addition of oxygen (lipid peroxidation) resulting in even greater variety and diversification of lipid species. The role of oxidized phospholipids as modulators of chronic inflammation, particularly in atherosclerosis, has been widely discussed.[2,8,9] Recent reports indicate that oxidized phospholipids may act as ligands for receptors that detect conserved pathogen-associated molecular patterns as an important part of innate immune defense. It is believed that the diversity of individual phospholipid oxidation products reflects their involvement in the regulation of many aspects of the inflammatory processes.[2,10−12]

Received: July 30, 2012
Revised: October 26, 2012
Published: November 13, 2012

dx.doi.org/10.1021/bi301024e | *Biochemistry* 2012, 51, 9736−9750

Further diversification of oxidatively modified phospholipid species may be achieved via their hydrolysis by either phospholipase A_1 (PLA_1) or phospholipase A_2 (PLA_2), each of which cleaves fatty acids from the *sn*-1 or *sn*-2 position of the glycerol backbone, respectively. The hydrolysis yields two types of products, free fatty acids (FFA) and lyso-phospholipids (lyso-PLs), that may also contain oxygenated functionalities. Polyunsaturated nonoxidized and oxygenated FFA and their metabolites released from phospholipids are well-recognized precursors of signaling molecules such as lipoxins, protectins, and resolvins, significant players in the resolution of inflammation.[3,13] Linoleic acid and its oxidized metabolites, abundant in LDL and atherosclerotic plaques, can act as regulators of macrophage differentiation and atherogenesis.[14,15] Notably, in mammalian cells, polyunsaturated fatty acids, especially linoleic acid, can be located in both *sn*-1 and *sn*-2 positions of phosphatidylethanolamine and PS.[7] Lyso-PLs (1-acyl-2-lyso-PL or 2-acyl-1-lyso-PL) can also exhibit signaling capabilities, for example, through interaction with G protein-coupled receptors (GPR34) on target cells.[16,17] Substantial concentrations of polyunsaturated lyso-phosphatidylcholine (lyso-PC, such as linoleoyl-lyso-PC and its hydroxy derivatives) can accumulate in the heart and human plasma.[10,11,18]

In the 1970s and 1980s, comparative assessments of the rates of PLA_2-catalyzed hydrolysis of "peroxidized" versus intact phospholipids in membranes documented a higher PLA_2 activity toward membranes and liposomes enriched with oxidatively modified lipids.[19−21] More recently, a Ca^{2+}-independent lipoprotein-associated phospholipase A_2 (Lp-PLA_2), also known as platelet-activating factor acetylhydrolase or type VIIA PLA_2, actively secreted by monocyte-derived macrophages, has been shown to preferentially hydrolyze oxidatively modified phospholipids, particularly phosphatidylcholines (PC).[22−24] The enzyme is associated with circulating LDL in humans and with macrophages within atherosclerotic plaques and catalyzes the formation of lyso-PC and oxygenated FFA.

Although PS comprises a relatively minor fraction of membrane phospholipids, its regulatory functions are central to cell activity.[25] The clearance of apoptotic cells by professional phagocytes is largely dependent on the ability of the latter to recognize PS as well as its oxidation products on the surface of apoptotic cells.[26−33] The possibility of hydrolysis of externalized PS or its oxidation products and the role of this in the recognition of apoptotic cells by professional phagocytes and inflammatory response have not been considered. Interestingly, activation of a secretory PS-specific PLA_1 was detected at various sites of inflammation and has been implicated in eicosanoid production.[34,35] However, the substrate specificity of PLAs toward different molecular species of peroxidized PS and their hydrolysis products has been insufficiently studied.

In this work, we performed liquid chromatography−mass spectrometry (LC−MS)-based structural characterization of oxygenated/hydrolyzed molecular species of PS-containing linoleic acid in either the *sn*-2 position ($C_{18:0}/C_{18:2}$, SL-PS) or both *sn*-1 and *sn*-2 positions ($C_{18:2}/C_{18:2}$, LL-PS), formed in the cytochrome *c* (cyt *c*)-driven enzymatic reaction in the presence of H_2O_2. Cyt *c* has been chosen as a catalyst of peroxidation reactions because of its likely involvement in PS oxidation in apoptotic cells.[29,36,37] Oxidation of SL-PS and LL-PS yielded oxygenated molecular species containing hydroxy, hydroperoxy, dihydroxy, hydroxy/hydroperoxy, and dihydroperoxy groups at different carbon atoms (C_8, C_9, and C_{12}−C_{14}) of linoleic acid at the *sn*-2 position. Further, LL-PS containing oxygenated linoleic acid at the *sn*-1 position with one and two oxygens was detected. Small amounts of oxidatively fragmented (truncated) PS molecular species were also generated. Lp-PLA_2 catalyzed the hydrolysis of both nontruncated and truncated species of oxidized PS, albeit with different efficiencies. Computer modeling of interactions of Lp-PLA_2 with oxidized species of PS indicated that they bind in the proximity (<3 Å) of a catalytic triad active site residue Ser273, favoring the hydrolysis of their *sn*-2 ester bond.

MATERIALS AND METHODS

Reagents. 1,2-Dioleoyl-*sn*-glycero-3-phosphocholine (DOPC), 1-stearoyl-2-linoleoyl-*sn*-glycero-3-phospho-L-serine (SL-PS), 1,2-linoleoyl-*sn*-glycero-3-phospho-L-serine (LL-PS), 1,2-diheptadecanoyl-*sn*-glycero-3-phospho-L-serine (PS, $C_{17:0}/C_{17:0}$), 1-stearoyl-2-hydroxy-*sn*-glycero-3-phospho-L-serine ($C_{18:0}$-lyso-PS), and 1-tridecanoyl-2-hydroxy-*sn*-glycero-3-phospho-L-serine ($C_{13:0}$-lyso-PS) were purchased from Avanti Polar Lipids Inc. (Alabaster, AL) and were of the highest purity available. Recombinant human lipoprotein-associated phospholipase A_2 (Lp-PLA_2) was obtained from GlaxoSmithKline Co. (Collegeville, PA). Cyt *c*, diethylenetriaminepentaacetic acid, DTPA, PLA_1 from *Thermomyces lanuginosus*, H_2O_2, and all organic solvents [high-performance liquid chromatography (HPLC) grade] were purchased from Sigma-Aldrich (St. Louis, MO). High-purity lyso-PS molecular species were obtained after their hydrolysis by porcine pancreas PLA_2 (Sigma-Aldrich) and subsequent separation by two-dimensional HPTLC. HPTLC silica G plates were purchased from Whatman (Schleicher & Schuell). Heptadecanoic acid ($C_{17:0}$) was obtained from Matreya LLC (Pleasant Gap, PA). 9(*S*)-Hydroperoxy-10(*E*),12(*Z*)-octadecadienoic acid, 9(*S*)-hydroxy-10(*E*),12(*Z*)-octadecadienoic acid, 13-oxo-9(*Z*),11(*E*)-octadecadienoic acid, 13(*S*)-hydroxy-9(*Z*),11(*E*)-octadecadienoic acid, 13(*S*)-hydroperoxy-9(*Z*),11(*E*)-octadecadienoic acid, 9(*S*)-hydroxy-10(*E*),12(*Z*)-octadecadienoic-9,10,12,13-d_4 acid, 9(10)epoxy-12(*Z*)-octadecenoic acid, and 12(13)epoxy-9(*Z*)-octadecenoic acid were purchased from Cayman Chemical Co. (Ann Arbor, MI).

Oxidation of Phosphatidylserine. DOPC/PS (500 μM, at a ratio of 1:1) liposomes were prepared by sonication in 50 mM HEPES buffer in the presence of 100 μM DTPA (pH 7.4). Liposomes containing PS (250 μM) were incubated with cyt *c* (5 μM) and H_2O_2 (100 μM) for 30 min or 3 h at 37 °C. At the end of the incubation, lipids were extracted by the Folch procedure[38] with minor modifications.

Phospholipid Hydrolysis by Lp-PLA_2. Liposomes containing DOPC and PS were treated with Ca^{2+}-independent secreted Lp-PLA_2 (0.26−2.6 μg of protein/sample) in 50 mM HEPES (pH 8.2) containing 100 μM DTPA for 30 min at 37 °C. After incubation with Lp-PLA_2, lipids were extracted and used for structural analysis by liquid chromatography−electrospray ionization mass spectrometry (LC−ESI-MS).

Phospholipid Hydrolysis by PLA_1. Liposomes containing DOPC and PS were treated with PLA_1 (2.4−24 μg of protein/sample) in 50 mM HEPES (pH 7.4) containing 100 μM DTPA for 30 min at 37 °C. After incubation with PLA_1, lipids were extracted and used for structural analysis by LC−ESI-MS.

LC−ESI-MS Analysis. This process was performed on a Dionex HPLC system (utilizing the Chromeleon software) consisting of a Dionex UltiMate 3000 mobile phase pump,

dx.doi.org/10.1021/bi301024e | *Biochemistry* 2012, 51, 9736−9750

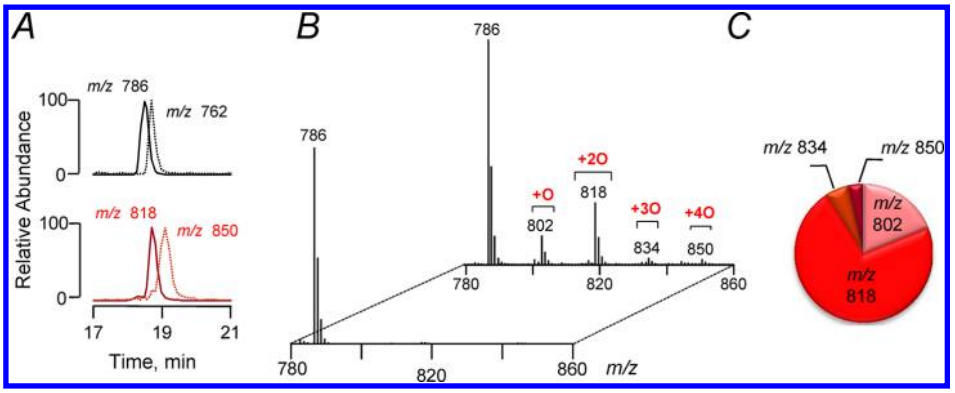

Figure 1. LC−ESI-MS detection and structural characterization of SL-PS oxidation molecular species formed in the cyt *c*-driven reaction in the presence of H_2O_2. (A) Typical reconstructed LC−ESI-MS profiles of nonoxidized (m/z 786) and oxidized (m/z 818 and 850) SL-PS molecular species that contained two and four oxygens, respectively. The peak at m/z 762 corresponds to internal standard PS ($C_{17:0}/C_{17:0}$). (B) MS^1 spectra of SL-PS before (front panel) and after its oxidation over 30 min induced by cyt *c* and H_2O_2 (back panel). Molecular ions corresponding to SL-PS containing one to four oxygens are detected on the MS spectrum. (C) Quantitative assessment of oxidized molecular species of SL-PS.

equipped with an UltiMate 3000 degassing unit, and UltiMate 3000 autosampler (sample chamber temperature set to 4 °C), and a 5 μL sample loop. The Dionex HPLC system was coupled to an ion trap mass spectrometer (FinniganTM LXQ with the Xcalibur operating system, Thermo Electron, San Jose, CA). The instrument was operated in the negative ion mode. For optimization of MS conditions and preparation of tune files, standards (2 pmol/μL) were injected by direct infusion through a syringe pump (flow rate of 10 μL/min) into the HPLC solvent flow (flow rate of 200 μL/min). The electrospray probe was operated at a voltage differential of 5.0 kV in the negative ion mode. The source temperature was maintained at 150 °C. Spectra were acquired in negative ion mode using full range zoom (m/z 400−1600 and 210−400 for FFA) scans. Tandem mass spectrometry (MS/MS analysis) of individual PS species was used to determine the fatty acid composition. MS^n analysis was conducted with a relative collision energy ranging from 20 to 40% and with an activation q value of 0.25 for collision-induced dissociation (CID) and a q value at 0.7 for the pulsed-Q dissociation (PQD) technique. MS/MS analysis was performed using an isolation width of m/z 1 and five microscans with a maximal injection time of 1000 ms. For selected reaction monitoring (SRM) experiments, the optimal collision energy was determined for each m/z parent−daughter ion pair (30 kV).

Normal Phase Column Separation of Phospholipids. Normal phase LC conditions were as described by Malavolta et al.[39] with slight modifications. Phospholipids (5 μL) were separated on a normal phase column [Luna 3 μm Silica (2) 100A, 150 mm × 2 mm (Phenomenex, Torrance, CA)] with a flow rate of 0.2 mL/min. The column was maintained at 30 °C. The analysis was performed using gradient solvents (A and B). Solvent A consisted of chloroform, methanol, and ammonium hydroxide (28%) [80:19.5:0.5 (v/v)]. Solvent B consisted of chloroform, methanol, water, and ammonium hydroxide [60:34:5:0.5 (v/v)]. The column was eluted during the first 3 min isocratically at 10% solvent B, from 3 to 15 min with a linear gradient from 10 to 37% solvent B, from 15 to 23 min with a linear gradient to 100% solvent B, from 23 to 45 min isocratically at 100% solvent B, and from 47 to 57 min isocratically at 10% solvent B for the equilibrium column. Reference standards of lyso-PS for LC−ESI-MS analysis were obtained after hydrolysis of SL-PS and LL-PS by PLA_2 and following their separation by two-dimensional HPTLC.

Reverse Phase Column Separation of Fatty Acids. FFA were separated on a reverse phase column [Luna 3 μm C_{18} (2) 100A, 150 mm × 2 mm (Phenomenex)] at a flow rate of 0.2 mL/min. The column was maintained at 30 °C. The analysis was performed using gradient solvents (A and B) containing 5 mM ammonium acetate. Solvent A consisted of tetrahydrofuran, methanol, water, and CH_3COOH [25:30:44.9:0.1 (v/v)]. Solvent B consisted of methanol and water [90:10 (v/v)]. The column was eluted during the first 3 min isocratically at 50% solvent B, from 3 to 23 min with a linear gradient from 50 to 98% solvent B, from 23 to 40 min isocratically using 98% solvent B, from 40 to 42 min with a linear gradient from 98 to 50% solvent B, and from 42 to 48 min isocratically using 50% solvent B for equilibration of the column.

Molecular Docking Studies. Three-dimensional structures of SL-PS, LL-PS, SL-PSox, and LL-PSox were generated using Marvin Sketch 5.3.6.[40] Hydroxy and hydroperoxy groups were placed at the *sn*-2 positions of SL-PS and LL-PS, yielding 9-hydroxy, 9-hydroperoxy, 9-hydroxy-14-hydroxy, 9-hydroxy-12,13-epoxy, 9-hydroperoxy-14-hydroperoxy, 13-hydroxy, and 13-hydroperoxy species. Oxidatively fragmented PS species containing either oxo or carboxy groups at the C_9 position (the end of truncation) were also created. These different species of oxidized PS were docked to the crystal structure of Lp-PLA_2 [Protein Data Bank (PDB) entry 3F9C] using AutoDock Vina[41,42] available at http://vina.scripps.edu. The lipid and Lp-PLA_2 three-dimensional structures were converted from pdb into pdbqt format using MGL Tools.[43] The Lp-PLA_2 structure was treated as the receptor and was kept rigid during docking. In contrast, rotatable bonds in the lipid structures imparted flexibility to the ligands. A grid box was centered at coordinates −14.59, −9.92, and −32.08 with 70 Å units in the x, y, and z directions, respectively, to cover the active site of Lp-PLA_2. Support for the chosen location of the grid box comes from a prediction of putative binding pockets by using Pocket-Finder (http://www.modelling.leeds.ac.uk/pocketfinder). Using this independent approach, the active site was predicted to be the largest putative ligand binding site. Docking with Autodock Vina[42] resulted in nine lowest-energy conformations. Of these conformations, we concentrated on those binding poses in which the *sn*-2 ester bond of the acyl chain was found in the proximity of the active site. For docking purposes, proximity was defined as a distance of <5 Å to either Ser273 or His315 of the catalytic triad.

Table 1. Structural Characterization of Nonoxidized and Oxidized SL-PS Molecular Species[a]

Parent ion, $[M-H]^-$	$[M-H\text{-serine}]^-$	$[M\text{-serine-}R^1CH_2COOH]^-$	$[M\text{-serine-}R^2CH_2COOH]^-$	$[FA-H]^-$ *sn*-1	$[FA-H]^-$ *sn*-2	Possible structure
786	699	415	419	283	279	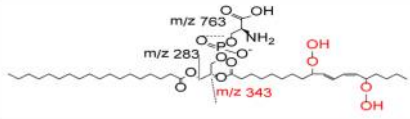
802	715	431	419	283	295	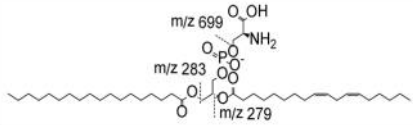
818	731	447	419	283	311	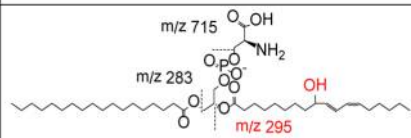
834	747	463	419	283	327	
850	763	479	419	283	343	

[a]SL-PS was analyzed by LC−ESI-MS using PQD mode. Chemical structures of five SL-PS regioisomers and their characteristic fragments with the indicated positions of the hydroxy or hydroperoxy groups on the side chain are shown. Structural ESI-MS analysis of nonhydrolyzed SL-PS in negative mode revealed deprotonated $[M - H]^-$ ions at m/z 786. The peak at m/z 699 is formed during fragmentation of PS (m/z 786) because of the loss of the serine group (residues 786 and 87). Molecular ions corresponding to stearic and linoleic acids at m/z 283 and 279, respectively, were detected in the MS spectrum as well. Fragments of $[M - \text{serine} - RCH_2COOH]^-$ corresponding to m/z values of 415 and 419 were identified as daughter ions without fatty acid from the *sn*-1 and *sn*-2 positions, respectively. MS^2 fragmentation of oxygenated SL-PS revealed the appearance of peaks at m/z 715, 731 747, and 763 formed due to the loss of the serine group (residues 802 and 87, 818 and 87, and 834 and 87). Ions at m/z 419 formed after the loss of oxidized linoleic acid are detected in the MS spectra. The appearance of carboxylate anions at m/z 295, 311, and 327 indicated that oxidized acyl chains from the *sn*-2 position of the glycerol backbone were also detected on MS^2 spectra. Detailed MS^2 analysis demonstrated that the PS $[M - H]^-$ ions at m/z 802, 818, 834, and 850 corresponded to PS species $C_{18:0}/C_{18:2}$+O, $C_{18:0}/C_{18:2}$+2O, $C_{18:0}/C_{18:2}$+3O, and $C_{18:0}/C_{18:2}$+4O, respectively.

RESULTS

Structural Characterization of Oxidized SL-PS Molecular Species Generated by Cyt *c* and H_2O_2. We characterized cyt *c*- and H_2O_2-catalyzed oxidation of two PS species, SL-PS, and LL-PS, containing nonoxidizable stearic acid ($C_{18:0}$) in the *sn*-1 position and oxidizable linoleic acid ($C_{18:2}$) in the *sn*-2 position, or linoleic acid in both *sn*-1 and *sn*-2 positions. A complex mixture of oxidation products, containing one, two, three, or four oxygens, was documented by LC−MS profiles (Figure 1A), MS^1 (Figure 1B), and MS^2 spectra (data not shown) of SL-PSox. Peroxidation of SL-PS (30 min at 37 °C) resulted in the formation of several oxygenated products at m/z 802, 818, 834, and 850 corresponding to the $C_{18:0}/C_{18:2}$+O, $C_{18:0}/C_{18:2}$+2O, $C_{18:0}/C_{18:2}$+3O, and $C_{18:0}/C_{18:2}$+4O species, respectively (Figure 1C). Detailed MS^2 analysis demonstrated that the PS $[M - H]^-$ ions at m/z 802, 818, 834, and 850 contained monohydroxy, monohydroperoxy, dihydroxy, and dihydroperoxy groups, respectively, attached to either C_9 or C_{13} of linoleic acid (Table 1). Oxygenated molecular species of SL-PSox with m/z 800 containing oxidized isomers of 9-oxo- and 13-oxo-linoleic acid were also observed (data not shown). The molecular species with two oxygens (m/z 818), corresponding to $C_{18:0}/C_{18:2}$+2O, was dominant, and its amount was estimated to be 9.4 ± 1.0 mol % of SL-PS.

Structural Characterization of SL-PSox Molecular Species Formed after Hydrolysis of Oxidized PS by Lp-PLA_2. DOPC liposomes containing oxidized species of either SL-PS or LL-PS were treated with human recombinant Lp-PLA_2, and the hydrolysis products were analyzed by LC−ESI-MS. Typical LC−ESI-MS base profiles of lyso-PS formed during hydrolysis of SL-PS with Lp-PLA_2 are presented in panels a and b of Figure 2A. Hydrolysis of SL-PS by Lp-PLA_2 yielded nonoxidized 1-stearoyl-2-lyso-PS (m/z 524) (Figure 2A, a−c) and a mixture of free linoleic acid (m/z 279) along with a wide spectrum of its oxygenated metabolites (Figure 3A,

dx.doi.org/10.1021/bi301024e | Biochemistry 2012, 51, 9736−9750

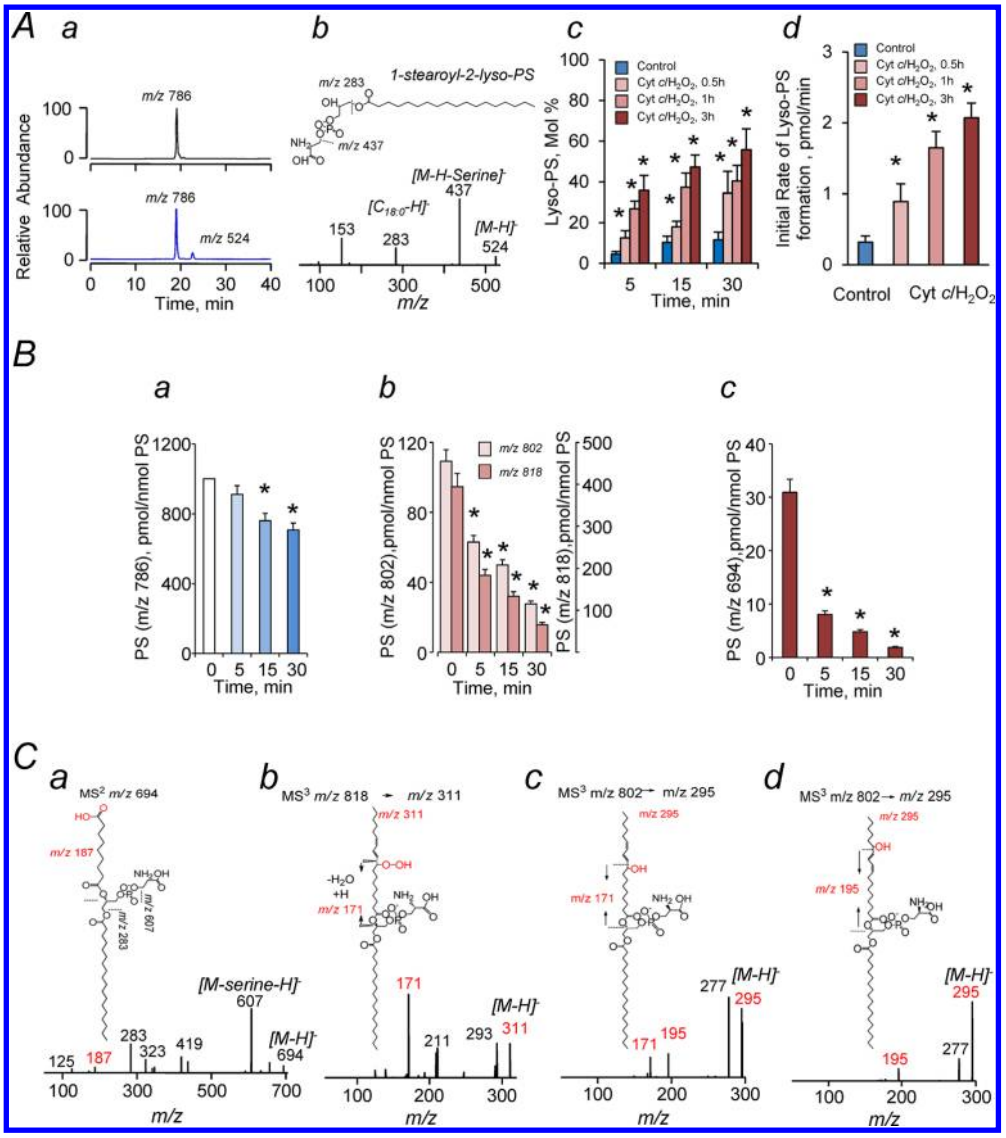

Figure 2. LC–ESI-MS detection and structural characterization of products formed after Lp-PLA$_2$-catalyzed hydrolysis of oxidized SL-PS. (A) (a) Typical normal phase LC–ESI-MS profiles of SL-PS before and after hydrolysis by Lp-PLA$_2$ (top and bottom, respectively). (b) MS^2 spectrum of lyso-PS molecular species formed after the hydrolysis and characteristic fragments of lyso-PS (m/z 524) (bottom) with its chemical structure (top). (c) Quantitative assessment of 1-acyl-2-lyso-PS formed after hydrolysis of nonoxidized (control) and oxidized (by cyt c and H_2O_2, after 0.5, 1, and 3 h) SL-PS at different time points. (d) Initial rate of nonoxidized and oxidized SL-PS hydrolysis by Lp-PLA$_2$. Each value represents the mean ± the standard deviation of at least three separate experiments. (B) Quantitative assessment of nonoxidized (a) and oxidized (by cyt c and H_2O_2, after 3 h) individual SL-PS species (b and c) during hydrolysis by Lp-PLA$_2$. Note that the efficiency of Lp-PLA$_2$ in hydrolyzing SL-PSox species was proportional to the amount of oxygen present in the acyl chains. Oxidatively truncated species were preferable substrates for Lp-PLA$_2$. (C) (a) Typical MS^2 spectrum of the parent ion at m/z 694 corresponding to oxidatively fragmented ON-PS molecular species. The inset shows the chemical structure and MS^2 fragmentation patterns of a molecular ion at m/z 694. (b) Typical MS^3 spectrum of a daughter ion at m/z 311 formed during fragmentation of a parent ion at m/z 818 corresponding to 9(S)-hydroperoxy-SL-PS molecular species. The inset shows the chemical structure and MS^3 fragmentation patterns of the molecular ion at m/z 818. (c) Typical MS^3 spectrum of the daughter ion at m/z 295 formed during fragmentation of the parent ion at m/z 802 corresponding to hydroxy-SL-PS molecular species. The inset shows the chemical structure and MS^3 fragmentation patterns of the molecular ion at m/z 802. (d) Typical MS^3 spectrum of the daughter ion at m/z 295 formed during fragmentation of the parent ion at m/z 802 after hydrolysis of hydroxy-SL-PS molecular species by Lp-PLA$_2$. The inset shows the chemical structure and MS^3 fragmentation patterns of the molecular ion at m/z 802. In this series of experiments, SL-PS was oxidized over 3 h. Note in panels a and d that fragments at m/z 171 and 195 corresponding to 9- and 13-oxygenated carboxylate anions of linoleic acid, respectively, were detected in the MS^3 spectrum of SL-PSox (m/z 802 > m/z 295). Hydrolysis of SL-PSox by Lp-PLA$_2$ results in elimination of the fragment at m/z 171 from the MS^3 spectrum; only the fragment at m/z 195 was observed in the in MS^3 spectrum obtained from the parent ion at m/z 802. Thus, hydrolysis of SL-PSox by Lp-PLA$_2$ results in the selective release of oxidized linoleic acid corresponding to C$_9$-hydroxy molecular species.

a). In line with previous reports,[19−21] significantly higher contents of hydrolysis products were found in the presence of peroxidized molecular PS species than with nonoxidized PS (Figure 2B, a–c). We found that Lp-LA$_2$-driven accumulation of lyso-PS was dependent on the duration of the incubation with the enzyme (Figure 2A, c). Further, the hydrolysis rate increased proportionally with the increased level of SL-PS oxidation (Figure 2A, d), whereby oxidatively truncated species were preferable substrates for Lp-PLA$_2$ (Figure 2B, c). Under our experimental conditions, no hydrolysis of nonoxidized

dx.doi.org/10.1021/bi301024e | Biochemistry 2012, 51, 9736–9750

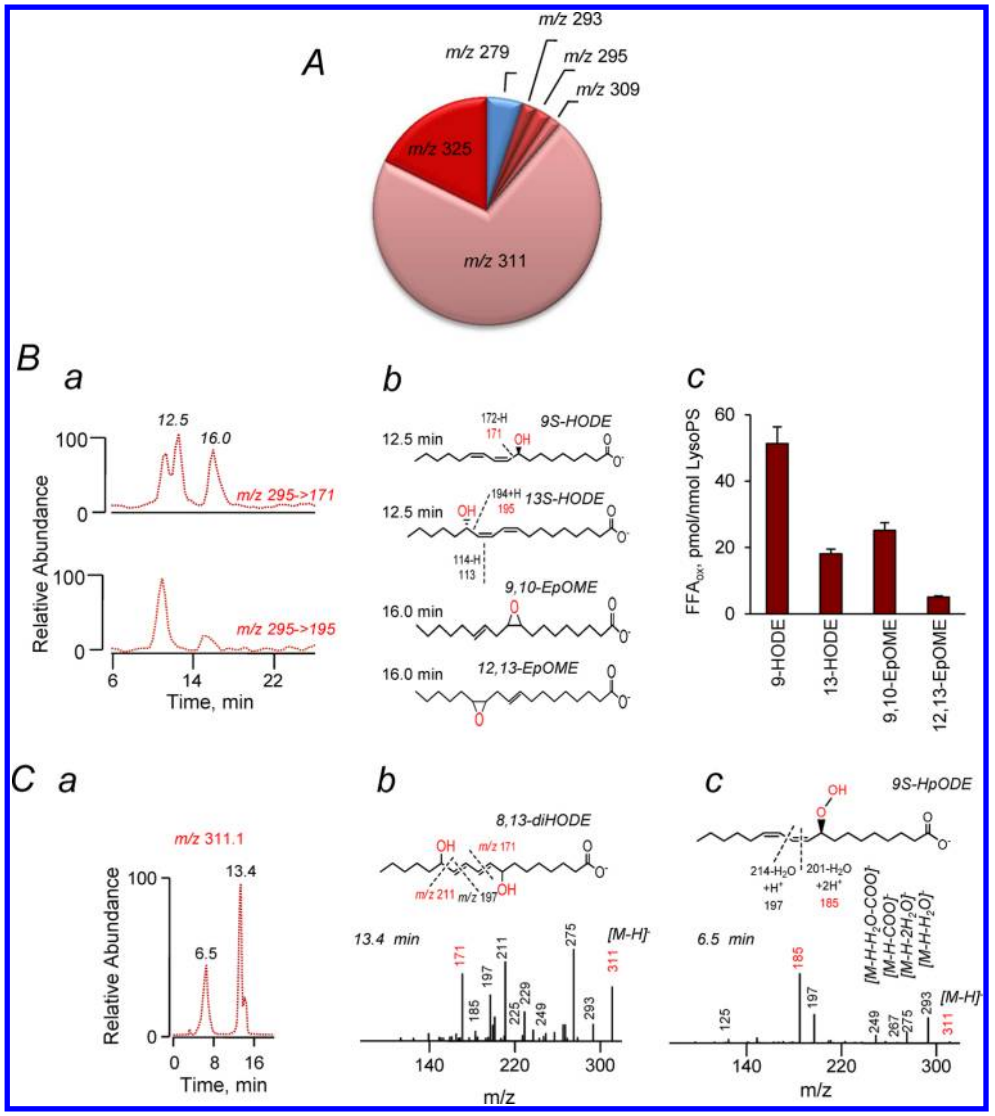

Figure 3. Structural characterization of FFA released from SL-PS after its hydrolysis by Lp-PLA$_2$. (A) Quantitative assessment of fatty acids released from SL-PS after its hydrolysis by Lp-PLA$_2$. (B) (a) Typical reverse phase LC−ESI-MS reconstructed profiles of the SRM for m/z 295 with appropriate mass transitions as noted are shown in the top (m/z 295 > m/z 171) and bottom panels (m/z 295 > m/z 195). (b) FFA chemical structures with the possible position of the oxygenated group on the side chain are shown. Peaks with retention times of 11−12 min correspond to 9(*S*)-HODE (m/z 171) and 13(*S*)-HODE (m/z 195), respectively. Peaks with retention times of 16 min correspond to 9,10-epoxy-C$_{18:2}$ (m/z 171) and 12,13-epoxy-C$_{18:2}$ (m/z 195), respectively. (c) Quantitative assessment of hydroxy- and epoxylinoleic acids released from SL-PS after its hydrolysis by PLA$_2$. (C) (a) Typical reverse phase LC−ESI-MS reconstructed profiles of free oxidized linoleic acid at m/z 311 formed after hydrolysis of SL-PSox by Lp-PLA$_2$. (b and c) MS^2 spectra (bottom) (C$_{18:2}$-OO, retention times of 6.5 and 13.4 min, respectively) at m/z 311 formed after hydrolysis of SL-PSox by Lp-PLA$_2$ and chemical structures (top) with the possible position of the oxygenated group on the side chain.

DOPC was observed. This is consistent with the exclusive role of PS, compared to other classes of phospholipids, as an activator of PLA$_2$.[44] Expectedly, PLA$_1$-induced hydrolysis of peroxidized SL-PS caused the release of stearic acid (m/z 283) and a mixture of lyso-PS with nonoxygenated (m/z 520) and oxygenated linoleic acid (m/z 534, 536, 550, 552, 566, 568, and 584) (data not shown).

The efficiency of Lp-PLA$_2$ hydrolysis of PSox species was proportional to the amount of oxygens present in the acyl chains (Figure 2B, c) and increased in the following order: SL-PS (m/z 786) ≪ SL-PSox (m/z 802) < SL-PSox (m/z 818) < SL-PSox (m/z 834) ≪ SL-PSox (m/z 694). Quantitatively, the amounts of hydrolyzed SL-PS corresponded to the accumulated lyso-PS species. Because oxidatively fragmented PC species have been reported as substrates for Lp-PLA$_2$,[45] we were eager to examine the effectiveness of the enzyme toward truncated species of PSox. To this end, we increased the incubation time (up to 3 h) for DOPC/SL-PS liposomes in the presence of cyt *c* and H_2O_2. This resulted in the significantly increased amounts of the major oxidized SL-PS species at m/z 818 (up to 40 mol % of PS) and simultaneously in the appearance of relatively small amounts of oxidatively fragmented PS molecular species at m/z 678 and 694 corresponding to 1-stearoyl-2-(9-oxononanoyl)-*sn*-glycero-3-phosphoserine (ON-PS, 1 mol % of PS) and 1-stearoyl-2-azelayl-*sn*-glycero-3-phosphoserine (A-PS, 3 mol % of PS). In spite of their low abundance, these truncated PSox species were hydrolyzed with higher efficiency than other oxidized PS species (Figure 2B, c). We further performed MS^3 analysis to determine which of the oxidatively modified PS acyls, oxygenated at the C$_9$ or C$_{13}$ atom, is a

dx.doi.org/10.1021/bi301024e | *Biochemistry* 2012, 51, 9736−9750

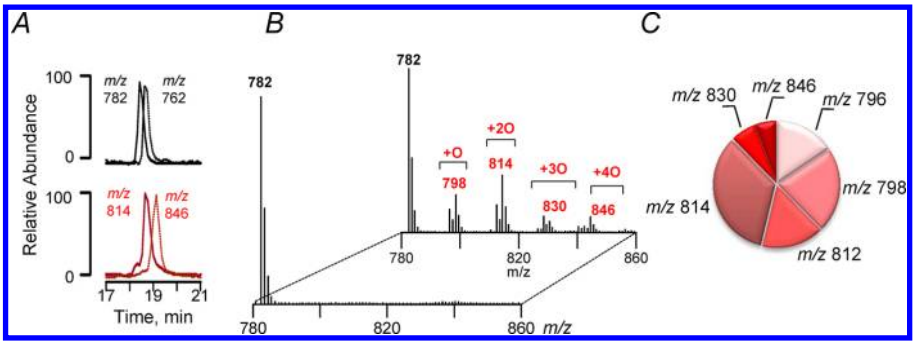

Figure 4. LC−ESI-MS detection and structural characterization of LL-PS oxidation molecular species formed in the cyt *c*-driven reaction in the presence of H_2O_2. (A) Typical reconstructed LC−ESI-MS profiles of nonoxidized (*m*/*z* 782) and oxidized (*m*/*z* 814 and 846) LL-PS molecular species that contained two and four oxygens, respectively. The Peak at *m*/*z* 762 corresponds to internal standard PS ($C_{17:0}/C_{17:0}$). (B) MS^1 spectra of LL-PS before (front panel) and after (back panel) its oxidation over 30 min induced by cyt *c* and H_2O_2. Molecular ions corresponding to SL-PS containing one to four oxygens are detected on the MS spectrum. (C) Quantitative assessment of oxidized molecular species of LL-PS.

preferable substrate for the enzyme. MS^n analysis of non-truncated SL-PSox, at *m*/*z* 818 (Figure 2C, b) and *m*/*z* 802 (Figure 2C, c), showed preferential cleavage of fatty acid residues containing hydroperoxy and hydroxy groups at the C_9 position. This preference was also observed for the oxidatively fragmented species of PSox (Figure 2C, a). Accordingly, the remaining, nonhydrolyzed, SL-PSox (*m*/*z* 802) contained only 13-hydroxylinoleic acid at the *sn*-2 position (Figure 2C, d). The hydrolysis by Lp-PLA_2, while overall effective toward SL-PSox, was still not 100% complete.

Characterization of the released oxidatively modified linoleic acid derivatives revealed the presence of molecular ions at *m*/*z* 295 that were identified as 9-hydroxy- and 13-hydroxylinoleic acid and mixture of epoxy derivatives of 9,10-epoxy- and 12,13-epoxylinoleic acid (Figure 3B, a, and Figure 3B, b). The amount of 9-hydroxy isomers of linoleic acid hydrolyzed by Lp-LPA_2 was significantly larger (51.3 pmol/nmol of lysoPS, for SL-PS) than the amount of 13-hydroxy isomers (18.1 pmol/nmol of lysoPS) (Figure 3B, c). The same tendency was observed for 9,10-epoxy- and 12,13-epoxylinoleic acid (*m*/*z* 295) (25.2 and 5.3 pmol/nmol of lysoPS, respectively, for SL-PS) (Figure, 3B, c). Among the oxygenated FFA (with one oxygen), 9-oxo- and 13-oxolinoleic acid (*m*/*z* 293) were found (data not shown). Cleaved oxygenated linoleic acid containing two oxygens was represented by 9-hydroperoxylinoleic acid and a mixture of dihydroxy (8,13-, 9,14-, and 9-hydroxy and 12,13-epoxy) derivatives of linoleic acid (Figure 3C, a−c).

Structural Characterization of Oxidized LL-PS Molecular Species Generated by Cyt *c* and H_2O_2. Cyt *c*-driven oxidation of LL-PS yielded a large variety of oxidized species (Figure 4A,B and Table 2). LL-PS molecular species with oxidized linoleic acid residues containing one, two, three, and four oxygens at *m*/*z* 798, 814, 830, and 846, respectively, were detected in the MS spectra (Figure 4B). Quantitatively, significantly greater accumulation of oxidized products was found among modified molecular species of LL-PS than among those formed from SL-PS (Figure 4C). Expectedly, oxygenation of LL-PS occurred in both *sn*-1 and *sn*-2 positions, whereby oxygenated species with oxygen(s) at C_9 and C_{13} of linoleic acid were formed. Oxidation of linoleic acid at the *sn*-1 position was less pronounced compared with that localized at the *sn*-2 position. Interestingly, oxygenation at the *sn*-1 position was observed only after the addition of two oxygens at the *sn*-2 position in molecular species of LL-PSox (Table 2).

Structural Characterization of LL-PSox Molecular Species Formed after Hydrolysis of Oxidized PS by Lp-PLA_2. Typical LC−MS profiles of lyso-PS are presented in panels a and b of Figure 5A. Hydrolysis of oxidized LL-PS by Lp-PLA_2 revealed the presence of two types of lyso-PS products with either nonoxygenated (Figure 5B, a) or oxygenated linoleic acid at the *sn*-1 position (Figure 5B, b). Nonoxidized 1-linoleoyl-2-lyso-PS at *m*/*z* 520 represented a dominant product, with smaller amounts of oxygenated lyso-PS species containing only one and two oxygens in the fatty acid moieties (*m*/*z* 534 and 536 and *m*/*z* 550 and 552, respectively) (Figure 5B, c). The total amount of accumulated lyso-PS was 18.1 ± 1.3 mol % of LL-PS, whereby the contents of nonoxidized lyso-PS (1-linoleoyl-2-lyso-PS) and oxidized-lyso-PS (1-oxidized linoleoyl-2-lyso-PS) were estimated to be 13.5 ± 0.9 and 4.6 ± 0.3 mol % of LL-PS, respectively (Figure 5B, d). LL-PSox species were hydrolyzed with higher efficiency (Figure 5C, a), yielding higher contents of hydrolysis products of PSox (Figure 5C, b) compared with nonoxidized PS (Figure 5C, c).

Similar to that of SL-PSox, the preferable cleavage of oxygenated fatty acid residues containing hydroxy and hydroperoxy groups in the C_9 position was observed for LL-PSox (data not shown). Interestingly, among products of LL-PSox hydrolysis, "heavily" oxygenated linoleic acids with one to four oxygens at C_9 or C_{13} (*m*/*z* 293, 295, 309, 311, 325, 327, and 343) were detected (Figure 6A). MS^2 analysis of the liberated oxygenated linoleic acid revealed the presence of 9-hydroxy and 13-hydroxy (Figure 6B, a and b), 8,13-dihydroxy (Figure 6C, a and b), 9,14-dihydroxy (Figure 6C, a and c), and 9-hydroperoxy derivatives (data not shown). Quantitatively, the level of oxidized linoleic acid was significantly higher than the content of nonoxidized linoleic acid, whereby hydroperoxy molecular species were dominant. Overall, 170.1 ± 16.6 pmol of oxidized and nonoxidized linoleic acid per nanomole of LL-PS was released due to hydrolysis of oxidized LL-PS by Lp-PLA_2. The contents of released oxidized and nonoxidized linoleic acid were 154.4 ± 13.1 and 15.7 ± 2.7 pmol/nmol of LL-PS, respectively. These estimates are in good agreement with the data for Lp-PLA_2-catalyzed accumulation of lyso-PS (see above).

To further verify the localization of oxygenated linoleic acid residues generated by Lp-PLA_2 hydrolysis, we additionally utilized PLA_1. In this case, the hydrolysis of oxidized LL-PS caused the release of nonoxidized and oxidized linoleic acid (containing one and two oxygens only) (Figure 7A) and

dx.doi.org/10.1021/bi301024e | *Biochemistry* 2012, 51, 9736−9750

Table 2. Structural Characterization of Nonoxidized and Oxidized LL-PS Molecular Species[a]

Parent ion, $[M-H]^-$	$[M-H-serine]^-$	$[M-serine-R^1CH_2COOH]^-$	$[M-serine-R^2CH_2COOH]^-$	$[FA-H]^-$ *sn*-1	$[FA-H]^-$ *sn*-2	Possible structure
782	695	415	415	279	279	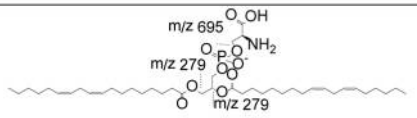
798	711	431	415	279	295	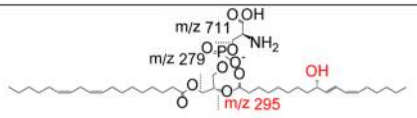
814	727	447	415	279	311	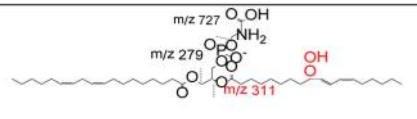
830	743	463	415	279	327	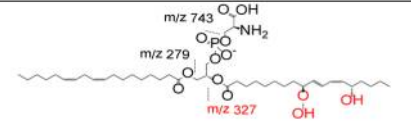
830	743	447	431	295	311	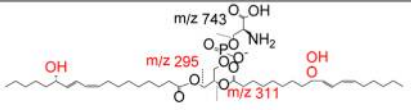
846	759	479	415	279	343	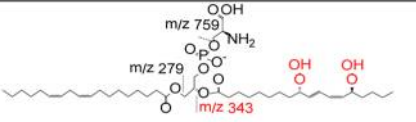
846	759	447	447	311	311	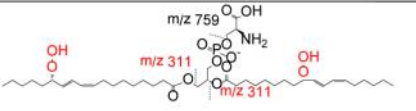

[a]Structural ESI-MS analysis of LL-PS in negative mode revealed deprotonated $[M - H]^-$ ions at m/z 782. The peak at m/z 695 formed after fragmentation of the PS molecular ion at m/z 782 was caused by the loss of the serine group (residues 782 and 87). In addition, fragmentation yielded two ions at m/z 415 via losses of $C_{18:2}$ from the molecular ion at m/z 695. The molecular ion at m/z 279 corresponding to the carboxylate anion of linoleic acid localized either at the *sn*-1 or at the *sn*-2 position of the glycerol backbone was also detected on the MS spectrum. MS^2 fragmentation of molecular ions corresponding to oxidized molecular species of LL-PS at m/z 798, 814, 830, and 846 revealed the appearance of peaks at m/z 711, 727, 743, and 759, respectively, formed due to the loss of the serine group (residues 798 and 87, 814 and 87, 830 and 87, and 846 and 87, respectively). Molecular ions at m/z 295, 311, 327, and 343 corresponding to oxygenated linoleic acid with one, two, three, and four oxygens, respectively, were also observed on MS spectra. The chemical structures of seven LL-PS regioisomers and their characteristic fragments utilized to characterize the position of the hydroxy or hydroperoxy groups on the side chain are shown.

oxidized species of lyso-PS containing oxygenated linoleic acid with one, two, three, and four oxygens (m/z 536, 552, 568, and 584, respectively) (Figure 7B). A lyso-PSox hydrolysis product with an ion at m/z 536 (containing 13-hydroxylinoleic acid with an ion at m/z 295) originated from two oxygenated molecular species of LL-PSox, one with an ion at m/z 814 [containing a trace amount of oxidized linoleic acid (m/z 295) at the *sn*-1 and *sn*-2 positions] and the other with an ion at m/z 830 [containing oxidized linoleic acid (m/z 295 and 311) at the *sn*-1 and *sn*-2 positions, respectively] (Figure 7C).

Molecular Modeling Studies of the Interaction of Lp-PLA_2 with Lipids Identified in This Study. In an effort to improve our understanding of the specificity of Lp-PLA_2 catalysis, we performed docking studies with a total of eight different species of PS and its oxidation products at different positions, including C_9, C_{13}, and C_{14}, as well as truncated species containing either oxo or carboxy groups at the C_9 position. Specifically, 9-hydroxy, 9-hydroperoxy, 9,14-dihydroxy, 9-hydroxy-12,13-epoxy, 9,14-dihydroperoxy, 13-hydroxy, 13-hydroperoxy, truncated C_9-oxo, and C_9-carboxy *sn*-2 species

dx.doi.org/10.1021/bi301024e | *Biochemistry* 2012, 51, 9736−9750

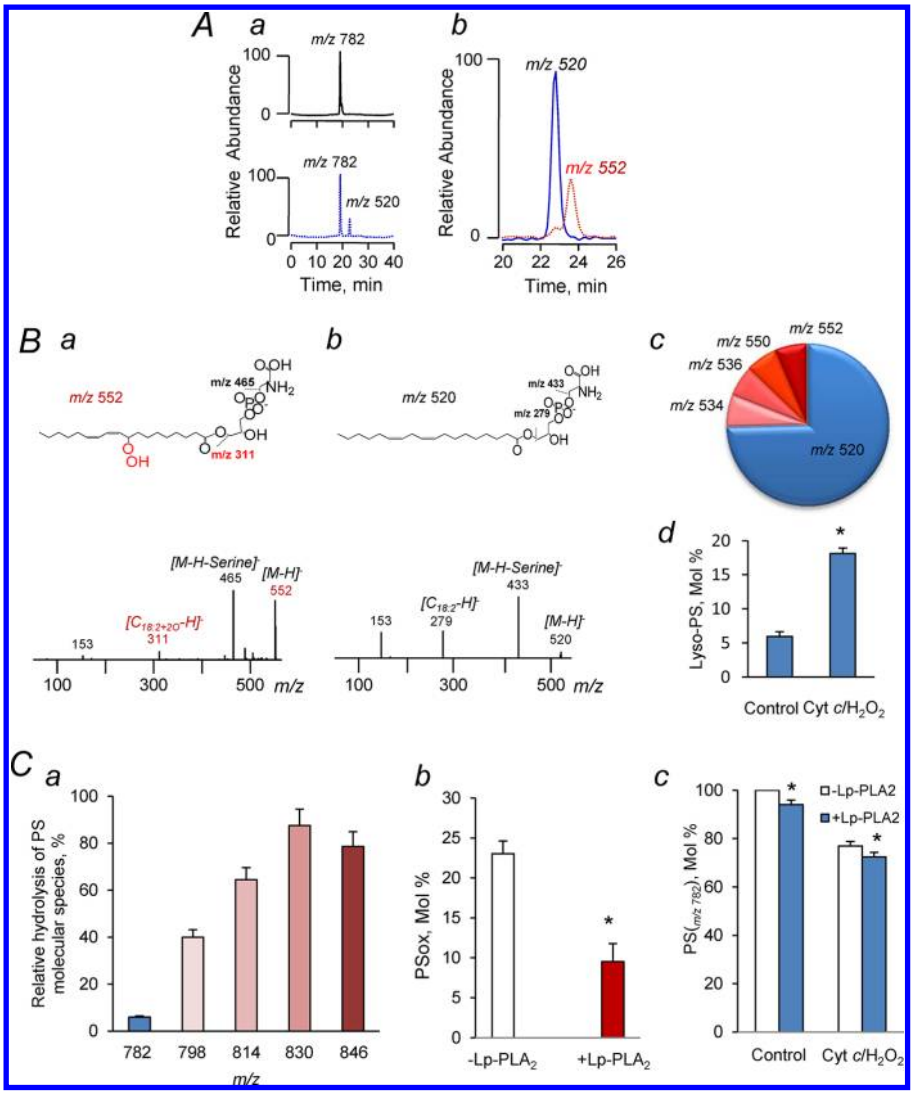

Figure 5. LC–ESI-MS detection and structural characterization of lyso-PS formed from LL-PS after hydrolysis by Lp-PLA$_2$. (A) Typical normal phase LC–ESI-MS profiles of LL-PS (a, top left) and 1-acyl-2-lyso-PS (a, bottom left, and b) formed after hydrolysis of LL-PS and LL-PSox by Lp-PLA$_2$. (B) MS^2 spectra of lyso-PS molecular species formed after its hydrolysis. Characteristic fragments of lyso-PS [*m*/*z* 552 (a, bottom) and *m*/*z* 520 (b, bottom)] and their chemical structures are shown (a and b, top panels). (c) Quantitative assessment of lyso-PS formed after hydrolysis of LL-PSox by Lp-PLA$_2$. (d) Quantitative assessment of 1-acyl-2-lyso-PS formed after hydrolysis of nonoxidized (control) and oxidized (cyt *c* and H_2O_2, 30 min) LL-PS (each value represents the mean ± the standard deviation of at least three separate experiments). (C) (a) Preferable hydrolysis of oxidized LL-PSox individual molecular species by Lp-PLA$_2$. The relative hydrolysis efficiency of individual SL-PS molecular species by Lp-PLA$_2$ is shown. (b) Quantitative assessment of oxidized LL-PS species during hydrolysis by Lp-PLA$_2$. (c) Quantitative assessment of nonoxidized LL-PS (*m*/*z* 782) before and after its incubation with cyt *c* and H_2O_2 during hydrolysis by Lp-PLA$_2$.

of both SL-PS and LL-PS were docked to the crystal structure of Lp-PLA$_2$ (PDB entry 3F9C, chain A)[41] to provide models for how different species interact with the protein that would help us gain mechanistic insight into the molecular basis for the experimental data obtained. The active site of Lp-PLA$_2$ is characterized by a catalytic triad composed of residues Ser273, Asp296, and His351 (Figure 8A), which accomplish hydrolysis of the *sn*-2 ester bond. Thus, we analyzed in detail those docking poses in which the *sn*-2 ester bond of the different oxidized species of SL-PS and LL-PS was located in the proximity (within 5 Å) of Ser273 and His351. In particular, we looked for poses in which the side chain O atom of Ser273 was close to the *sn*-2 carbonyl O atom and the *sn*-2 ester O atom faced the closest His251 N atom (Figure 8A, dashed lines). Table 3 lists the lowest binding energies, the numbers of poses satisfying this proximity criterion, and the above-mentioned distances to Ser273 and His351 for the different oxidized species. The binding poses corresponding to the C_9-oxo, C_9-carboxy, 9-hydroxy, 13-hydroperoxy, and 9,14-dihydroxy groups of SL-PS and the 9-hydroperoxy groups of both LL-PS and SL-PS species are shown in Figure 8. In most cases, the phospholipid headgroups of SL-PS and LL-PS bind close to a positively charged Lys370 (Figure 8). This residue was shown previously to play a role in binding of HDL[46] and LDL[47] to Lp-PLA$_2$. The OH group of the serine headgroup of PS in most cases points toward Lys370 (Figure 8B–D), although more rarely it points away from Lys370 (Figure 8E), albeit still in the proximity. This proximity, particularly when the serine headgroup is facing Lys370, leaves only one reasonable choice for the location of the *sn*-1 acyl chain, which is to be buried in a hydrophobic pocket (Figure 8). In general, the position of the *sn*-1 chain in the hydrophobic pocket is independent of the

dx.doi.org/10.1021/bi301024e | *Biochemistry* 2012, 51, 9736–9750

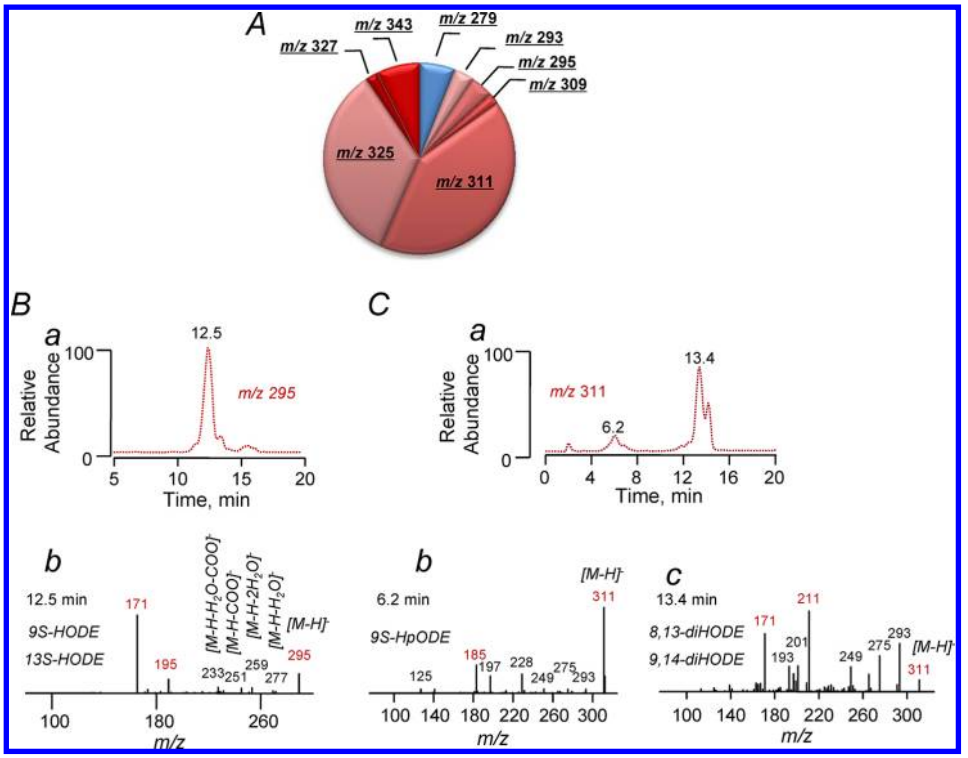

Figure 6. Structural characterization of free fatty acids released from LL-PS after their hydrolysis by Lp-PLA_2. (A) Quantitative assessment of fatty acids released from LL-PS after its hydrolysis by Lp-PLA_2. (B) Typical reverse phase LC−ESI-MS reconstructed profile (a) and MS^2 spectrum (b) of oxygenated linoleic acid (m/z 295) released after hydrolysis of LL-PSox by Lp-PLA_2. (C) Typical reverse phase LC−ESI-MS reconstructed profiles (a) and MS^2 spectra (b and c) of free oxidized linoleic acid ($C_{18:2}$-OO, retention times of 6.5 and 13.4 min, respectively) at m/z 311 formed after hydrolysis of LL-PSox by Lp-PLA_2.

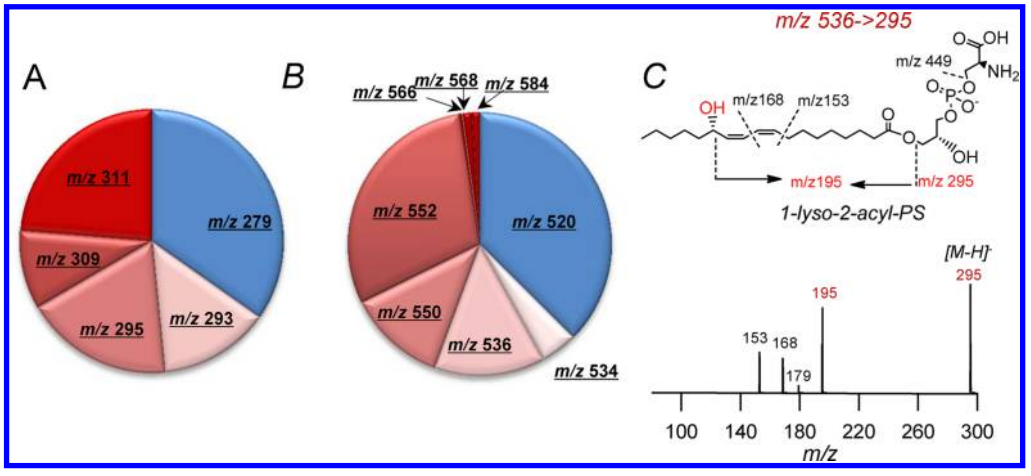

Figure 7. Structural characterization of free fatty acids released from LL-PS after their hydrolysis by PLA_1. (A) Quantitative assessment of FFA released from LL-PS after its hydrolysis by PLA_1. (B) Quantitative assessment of lyso-PS released from LL-PS after its hydrolysis by PLA_1. (C) MS^3 spectrum of oxidized lyso-PS molecular species with an ion at m/z 536 (bottom) and its possible chemical structure (top).

lipid species analyzed. The *sn*-1 acyl chain binding site is similar to the proposed platelet activating factor (PAF) binding site.[41]

What is the mechanism by which oxidized lipids bind in the proximity of the catalytic active site? Although the energies predicted for the different lipid species did not differ drastically, nonoxidized PS does bind less preferentially than oxidized species of both SL-PS and LL-PS (Table 3). Furthermore, a relatively larger number of conformations was observed in the proximity of the catalytic site (Table 3). A detailed analysis of the environment of the OH and OOH groups in the different high-ranking poses suggests that a number of interactions by these groups with the protein contribute favorably to binding (Table 4). In particular, OH and OOH groups were frequently observed to interact with aromatic residues in the binding pocket, in particular Phe322 (in contact in poses for *C_9-O, *C_9-OOH, 9-OOH, 9-OH-14-OH, 9-OOH-14-OOH) and Tyr324 (for *C_9-OOH, 9-OH, 9-OOH, 9-OH-14-OH, and 9-OOH-14-OOH), but sometimes Phe110 (for *C_9-OOH and 9-OH-14-OH), Tyr321 (9-OH-14-OH), or Trp298 (for *C_9-OOH and 9-OH-14-OH) was involved. Polar interactions also play a role in some conformations, such as with Arg218 (for *C_9-O, *C_9-OOH, and 9-OOH), Gln211 (for *C_9-O), and

dx.doi.org/10.1021/bi301024e | *Biochemistry* 2012, 51, 9736−9750

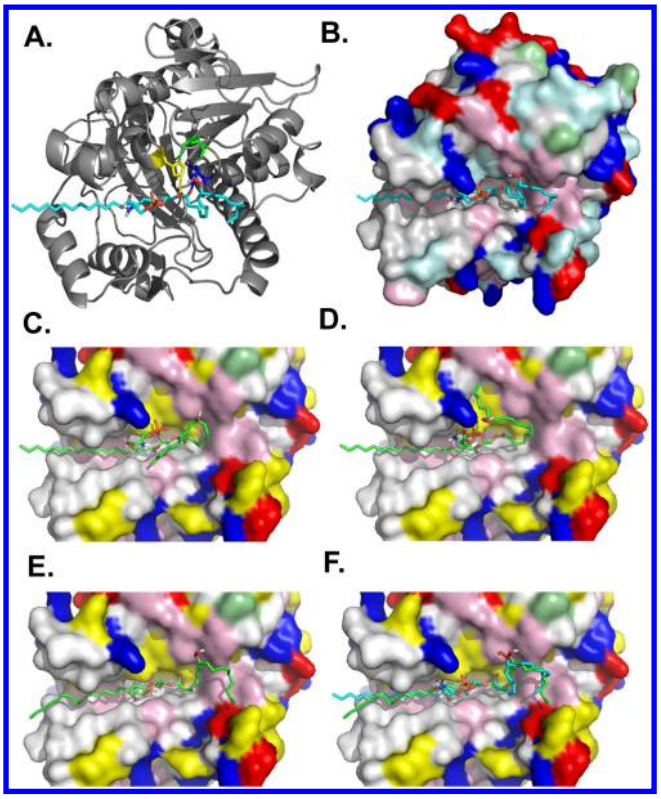

Figure 8. Molecular models of oxidized SL-PS and LL-PS bound to the crystal structure of Lp-PLA_2. (A) Cartoon representation of Lp-PLA_2 in complex with a hydroperoxy group at C_9 of SL-PS. The residues corresponding to the catalytic triad, Ser273, Asp296, and His351, are colored blue, green, and yellow, respectively, and rendered as sticks. The proximity of the Ser273 side chain O atom to the *sn*-2 carbonyl O atom and the His351 N atom to the *sn*-2 ester O atom is highlighted using blue and yellow dashes, respectively. Surface representations of Lp-PLA_2 with the predicted binding poses for hydroperoxy at C_9, hydroxyl at C_9, and hydroperoxy at C_{13} of SL-PS are shown in panels B–D, respectively. The predicted binding interface of the (E) hydroperoxy group at C_9 of LL-PS and (F) an overlay of the hydroperoxy group at C_9 for both SL-PS (with carbons colored cyan) and LL-PS species (with carbons colored green). The surface is colored on the basis of residue type in panels B–F. The residues corresponding to polar, hydrophobic, aromatic, positively charged, and negatively charged residues are colored yellow, white, magenta, blue, and red, respectively. SL-PSox and LL-PSox are rendered as sticks in all cases. The images were generated using PyMOL.[68]

Glu214 (for *C_9-O, *C_9-OOH, 9-OOH, and 9-OH-14-OH). There are also intramolecular interactions within the lipids observed, such as with the PS phosphate (*C_9-O, *C_9-OOH, 9-OH, and 9-OOH) or the PS amino group (9-OH-14-OH). Thus, the predicted stabilization of oxidized lipids through molecular contacts is in line with the known specificity of Lp-PLA_2 toward oxidized phospholipids[45] and provides mechanistic insight into the underlying reasons for the stabilization. Further, the *sn*-2 ester bond in both LL-PS and SL-PS was positioned in the proximity of both Ser273 and His351 in the case of oxidatively fragmented species at the C_9 position as compared to the C_{13} position (Table 3). This suggests that one should expect the truncated *sn*-2 species to be preferred substrates, followed by C_9-oxygenated nontruncated isomers, compared to C_{13} isomers, in line with the effectiveness of the hydrolysis of different oxidized PS species observed experimentally.

DISCUSSION

As a member of the PLA_2 superfamily, Lp-PLA_2 has a distinguishing characteristic that it is highly specific for the type of *sn*-2 residue to be hydrolyzed. In particular, phospholipid truncated oxidation products of the abundant *sn*-2 linoleoyl-containing phospholipids that harbor nine-carbon ω-aldehyde or carboxylate functions are efficiently hydrolyzed by the enzyme.[48] Because circulating Lp-PLA_2 is produced by inflammatory cells, is bound to lipoproteins, and accumulates in human atherosclerotic lesions, the role of the enzyme in the metabolism of oxidized PC species was the major focus of many studies.[22,45] Lp-PLA_2 effectively degrades oxidatively modified phospholipids present in oxidized LDL, particularly PCox, to yield two pro-inflammatory mediators, lyso-PC and oxidized nonesterified fatty acids, both of which may play a role in the development of atherosclerotic lesions and formation of a necrotic core, leading to more vulnerable plaques.[22,23,48−50] Recent work has documented the essential role of oxidatively truncated PC and its Lp-PLA_2 hydrolysis products in TNFα-induced cell death.[51] The biological role of Lp-PLA_2 in metabolic conversions of other oxidatively modified phospholipids, particularly of anionic phospholipids, was largely neglected. Among the latter, PS and its oxidation products have been identified as signals that are essential for prompt and selective removal of "unwanted" or harmful cells, including apoptotic cells, acting as apoptotic cell-associated molecular patterns (ACAMPs).[52] Recognition of PS-based ACAMPs by specific macrophage receptors is an intrinsic part of the "programmed clearance" of apoptotic cells at sites of inflammation that plays an important role in the resolution of the inflammatory process.[32]

Recently, we demonstrated that phospholipid peroxidation in vivo induced by a number of "oxidative stress"-inducing factors, e.g., γ-irradiation, hyperoxia, and traumatic brain injury, follows a specific nonrandom pattern in which two anionic phospholipids, a mitochondrion-specific cardiolipin (CL) and extramitochondrial PS, represent the major oxidation substrates. In contrast, more abundant and highly polyunsaturated PC and phosphatidylethanolamine are not involved in the peroxidation process.[53,54] We identified cyt *c* as a potent catalyst of these peroxidation reactions taking place in mitochondria early during the initiation of the cell death program and in extramitochondrial compartments later during the execution of apoptosis.[28] Biologically, these peroxidation reactions were related to two signaling functions: (i) participation of CL peroxidation products in mitochondrial membrane permeabilization[28] and (ii) involvement of PS peroxidation products in the externalization process and recognition of PS and oxidatively modified PS species by putative receptors of professional phagocytes.[26] Possible hydrolysis of peroxidized species of either CL or PS by PLAs and likely roles of the hydrolysis products in the regulation of apoptosis and phagocytosis have not been studied.

In this work, we employed LC–MS to characterize the hydrolysis pathways of Lp-PLA_2 toward peroxidized species of PS. For the first time, we demonstrated that oxidized PS can be used by Lp-PLA_2 as a substrate. Lp-PLA_2 is highly effective in catalyzing the hydrolysis of different nontruncated and truncated peroxidized species of SL-PSox and LL-PSox formed by cyt *c*- and H_2O_2-driven catalysis. Expectedly, oxygenated

Table 3. Parameters Obtained from Molecular Docking of Nonoxidized and Oxidized SL-PS and LL-PS Species to the Lp-PLA$_2$ Structure Using Autodock Vina (see Materials and Methods)[a]

	PS ($C_{18:0}/C_{18:2}$)			PS ($C_{18:2}/C_{18:2}$)		
sn-2 species	predicted binding energy (no. of conformations)	S273 (Å)	H351 (Å)	predicted binding energy (no. of conformations)	S273 (Å)	H351 (Å)
nonoxidized	−6.5 (1)	4.42	6.41	−6.2 (1)	4.5	4.42
*C_9-O	−7.3 (4)	2.75	3.33	−8.3 (3)	2.76	3.40
*C_9-OOH	−7.3 (6)	2.83	3.28	−7.3 (5)	2.77	3.07
-9-OH	−7.5 (3)	2.89	3.46	−7.5 (4)	2.90	3.26
-9-OOH	−7.4 (5)	2.89	3.13	−7.9 (6)	2.96	2.82
-9-OH-14-OH	−7.8 (5)	2.81	3.6	−7.3 (5)	2.77	3.48
-9-OOH-14-OOH	−6.8 (3)	3.17	3.09	−7.2 (5)	2.87	3.07
-9-OH-(12,13)-O	−6.8 (1)	2.98	4.28	−6.7 (1)	2.79	5.08
-13-OH	_[b]	_[b]	_[b]	_[b]	_[b]	_[b]
-13-OOH	−7.4 (1)	5.23	3.9	−6.2 (1)	4.07	5.42

[a]The reported score corresponds to the lowest binding energy in each case. The predicted binding energy in kilocalories per mole along with the total number of conformers bound in the proximity of the active site is provided in each case, i.e., for the SL-PS and LL-PS species and various SL-PSox and LL-PSox species. Furthermore, the distances from the Ser273 side chain O atom to the *sn*-2 carbonyl O atom and from the His251 N atom to the *sn*-2 ester O atom are listed for the conformation for which the distance was shortest. An asterisk denotes a truncated species. [b]None of the predicted binding poses for 13-OH were in the proximity of the active catalytic site of PLA$_2$. For this reason, no results are reported for 13-OH, based on our selection criteria as detailed in Materials and Methods.

Table 4. Amino Acids in the Proximity of OH and OOH Groups on Oxidized Lipids[a]

sn-2 species	contact residue(s) [conformation(s)]
*C_9-O	phosphate of PS [2,4], Phe322 [2,4], Arg218 [5], Gln211 [6], Glu214 [6]
*C_9-OOH	phosphate of PS [1,6], Phe322 [2], Arg218 [3], Glu214 [3], Phe110 [4], Tyr324 [5], Trp298 [5]
-9-OH	phosphate of PS [1], Tyr324 [2], none [3]
-9-OOH	phosphate of PS [1,2,3], Tyr324 [1,2,3], Phe322 [1,2,3], Glu214 [4], Arg218 [4], none [6]
-9-OH-14-OH	
-9-OH	amine of PS [1], Phe322 [1], Tyr321 [2], Glu214 [3], Trp298 [3], Tyr324 [4,6], Trp298 [6]
-14-OH	Phe110 [1], Leu111 [1], amine of PS [2], none [3,4], Glu214 [6]
-9-OOH-14-OOH	
-9-OOH	Phe322 [1], none [2], Tyr324 [3]
-14-OOH	Leu111 [1], none [2,3]

[a]Bound ligand conformations predicted by Autodock Vina are numbered according to their rank 1−9, and their identity is given in brackets after the contact residue. Only PS ($C_{18:0}/C_{18:2}$) was evaluated.

species of linoleic acid and nonoxidized stearoyl-lyso-PS constituted the major products of hydrolysis when SL-PSox was used as a substrate. Notably, 9-isomers of oxygenated linoleic acid were dominating as hydrolysis products. Further, hydroxy derivatives of linoleic acids, particularly the 9-hydroxy form, participate in regulatory pathways through interaction with the recently described receptor for long chain fatty acids, G2A. The receptor mediates intracellular signaling events such as intracellular calcium mobilization and JNK activation as well as the secretion of cytokines (interleukin-6 and -8); it also blocks cell cycle progression at the G1 phase in response to ligands.[55]

We also established that oxidation of doubly polyunsaturated PS resulted in the formation of PS polyoxygenated products with hydroperoxy and hydroxy groups located at both *sn*-1 and *sn*-2 positions. Lp-PLA$_2$ utilized 9-stereoisomers of peroxidized LL-PS as preferred substrates for the catalytic hydrolysis yielding 9-oxygenated derivatives of linoleic acid. Finally, Lp-PLA$_2$ is effective in the catabolism of oxidatively fragmented PSox species, in line with the previously demonstrated effectiveness of Lp-PLA$_2$ in hydrolyzing truncated oxidized PC species.[30,45,48] It is conceivable that both long chain oxygenated derivatives of linoleic acid and its truncated oxidatively modified fragments will be released by Lp-PLA$_2$. The yield of these respective products will be dependent on the relative abundance of different PS oxidation products that, in turn, is determined by specific peroxidation pathways. Considering that cyt *c* may be a major catalyst of PS oxidation under pro-apoptotic conditions, it is likely that oxygenated long chain fatty acid residues may dominate as the products of PS peroxidation. Detailed analysis of these PS peroxidation−hydrolysis products may lead to the identification of meaningful biomarkers of nonrandom oxidative stress in phospholipids.

To obtain molecular insights into the underlying mechanisms for the experimentally found selectivity in the hydrolysis of different lipid species, we investigated the structural basis for the interaction of Lp-PLA$_2$ with different oxidized and nonoxidized PS species. While a catalytic dyad with His and Asp residues has been identified in many PLA$_2$s, a catalytically essential Ser273 is present in two major cytosolic PLA$_2$s, GIVA and GVIA,[56] as well as in Lp-PLA$_2$. In the latter case, the active site is composed of a catalytic triad involving Ser, His, and Asp, whereby Ser273 acts as a nucleophile that attacks the *sn*-2 ester bond of phospholipids.[57] Thus, the arrangement of the *sn*-2 ester bond in the proximity of Ser273 might explain the specificity for differential hydrolyses observed experimentally for the different oxygenated molecular species. Especially for the SL-PSox and LL-PSox species with a hydroxy or hydroperoxy group at the C_9 position (9-hydroxy or 9-hydroperoxy, respectively), which are hydrolyzed preferentially, the *sn*-2 ester bond of these species is predicted to bind very close (<3 Å) to Ser273 compared to other species. Thus, the closer the oxygenated group is to the *sn*-2 ester bond of the species (i.e., oxygenation at C_9 is closer than that of C_{13}), the more amenable that species is to hydrolysis by Lp-PLA$_2$. While there are only subtle differences in the predicted energies between SL-PS and LL-PS, the conclusion that there is specificity of Lp-PLA$_2$ for C_9 versus C_{13} oxidized lipids from the observed experimental results and the proximity to Ser_{273} is

dx.doi.org/10.1021/bi301024e | *Biochemistry* 2012, 51, 9736−9750

further supported by the observation that multiple conformers are predicted to bind closer to the active site in the case of oxygenated species at the C_9 position than those at the C_{13} position, regardless of SL-PSox versus LL-PSox. These results are also in agreement with previous studies that indicated that Lp-PLA_2 can cleave oxidized lipids in the *sn*-2 position up to nine carbons long.[58]

To understand the mechanisms by which the *sn*-2 ester bond may be brought close to the active site, we investigated the different binding poses predicted by computer modeling. We find that the hydroxy and hydroperoxy groups in particular at the C_9 position bind in the proximity of aromatic residues that surround the binding pocket, especially Tyr324 and Phe322 (Figure 8B,C, aromatics are colored pink). These residues may participate in the stabilization of the interactions with these lipid species via OH donation by the oxidized lipids to π systems of surrounding aromatic residues in Lp-PLA_2. In the C_{13}-OOH case, but also in some poses obtained for the truncated C_9 species and in 9-OOH species, there is a stabilizing interaction with positive charges on Lp-PLA_2 (Figure 8D). These additional stabilizing interactions afforded by the oxidation groups position the *sn*-2 ester bond in oxidized species closer to the catalytic site, thus resulting in the experimentally observed preference observed in the hydrolysis of species with oxidation at the C_9 position by Lp-PLA_2. LC−MS experimental data indicate that truncated *sn*-2 species of oxidatively modified PS are better substrates for Lp-PLA_2 than respective long chain oxygenated species of PS, consistent with the computer modeling results.

Information about the possible involvement of oxidatively modified forms of PS and their metabolites in inflammation is starting to emerge. It has been shown that products of peroxidized PS hydrolysis, lyso-PS and oxygenated forms of linoleic acid, may act as signals by regulating anti- and pro-inflammatory responses.[14,15] However, MS-based analysis of peroxidation−hydrolysis products formed from PS has not been performed. Our findings of oxygenated forms of lyso-PS by which oxygenated fatty acid residues are located at either *sn*-1 or *sn*-2 positions suggest that these unusual PS species may also be involved in yet to be identified signaling pathways of apoptosis and phagocytosis, possibly contributing to the development of inflammation. In fact, macrophage receptors, such as scavenger receptors and other putative receptors of PS and PSox, that mediate uptake of oxidatively modified lipoproteins are also implicated in the recognition of apoptotic cells along with other known receptors, TIM-3, TIM-4, and G2A.[59,60] Interestingly, a recent study demonstrated a role for lyso-PS in enhancing the in vitro clearance of dying neutrophils via the G2A receptor.[31] It is noteworthy from the observations made in our studies that Lp-PLA_2 is capable of generating various ligands for the G2A receptor: HODEs, lyso-PS, and lyso-PC. Moreover, PS and lyso-PLs are tightly bound to human CD1 molecules (a family of β_2-microglobulin-associated glycoproteins) at the cell surface and are involved in recognition by T lymphocytes.[59] Interestingly, oxidatively modified PC species have been reported to induce an unusual macrophage phenotype (Mox) that has been associated with the severity of atherosclerotic lesions and chronic inflammation.[61] Surprisingly, the influence of PSox species externalized on the surface of apoptotic cells, which can be directly recognized by macrophages,[17,31,36] as well as their hydrolysis products as determinants of macrophage phenotype in pro-inflammatory environments remains poorly understood.

Free radical peroxidation of phospholipids has been notoriously qualified as one of the major mechanisms of membrane damage occurring in a number of disease conditions.[62] The widely accepted concept of oxidative stress, induced by excessive formation of ROS and other radical intermediates, has led to numerous clinical trials whose results and subsequent meta-analysis turned out to be less than satisfying.[8,63−65] The reasons for these disappointments may be associated with a poor understanding of the enzymatic catalytic mechanisms involved in the production of oxidative stress as well as with underappreciation of the specific signaling (rather than nonspecific deleterious) roles of oxidatively modified lipids. While the pathways triggered by PLA_2-driven release of eicosanoids, docosapentanoids, and docosahexanoids and their subsequent oxygenation by cyclooxygenases and lipoxygenases have been well characterized,[66,67] the role and biology of peroxidized phospholipids as precursors of biologically active molecules have been markedly less studied. Further investigations of the enzymatic metabolic pathways involved in the peroxidation of phospholipids and subsequent hydrolysis of their oxidized species leading to the production of important lipid regulators are important. For example, this work provides a reason to study the biological consequences of having apoptotic cells, together with their extracellular facing oxidized phospholipids, in close conjunction with secreted Lp-PLA_2 derived from its primary cellular source, the professional phagocyte, the activated macrophage.

AUTHOR INFORMATION

Corresponding Author

*V.A.T.: Center for Free Radical and Antioxidant Health, Department of Environmental and Occupational Health, University of Pittsburgh, Bridgeside Point, 100 Technology Dr., Suite 324, Pittsburgh, PA; telephone, (412) 383-5099; fax, (412) 624-9361; e-mail, vtyurin@pitt.edu. V.E.K.: Center for Free Radical and Antioxidant Health, Department of Environmental and Occupational Health, University of Pittsburgh, Bridgeside Point, 100 Technology Dr., Suite 350, Pittsburgh, PA; telephone, (412) 624-9479; fax, (412) 624-9361; e-mail, kagan@pitt.edu.

Funding

Supported by National Institutes of Health Grants HL70755, ES020693, ES021068, U19 AIO68021, and NS076511 and by National Institute for Occupational Safety and Health Grant OH008282

Notes

The authors declare no competing financial interest.

ABBREVIATIONS

A-PS, stearoyl-azelayl-phosphatidylserine; CL, cardiolipin; DTPA, diethylenetriaminepentaacetic acid; diHODE, dihydroxyoctadecadienoic acid; DOPC, dioleoylphosphatidylcholine; EpOME, epoxyoctadecenoic acid; FFA, free fatty acids; HpODE, hydroperoxyoctadecadienoic acid; HODE, hydroxyoctadecadienoic acid; Lp-PLA_2, lipoprotein-associated phospholipase A_2; LL-PS, dilinoleoylphosphatidylserine; lyso-PL, lyso-phospholipids; PC, phosphatidylcholine; PS, phosphatidylserine; ON-PS, stearoyloxononanoylphosphatidylserine; SL-PS, stearoyllinoleoylphosphatidylserine.

REFERENCES

(1) Dowhan, W. (1997) Molecular basis for membrane phospholipid diversity: Why are there so many lipids? *Annu. Rev. Biochem. 66*, 199−232.

(2) Furnkranz, A., and Leitinger, N. (2004) Regulation of Inflammatory Responses by Oxidized Phospholipids: Structure-Function Relationships. *Curr. Pharm. Des. 10*, 915−921.

(3) Bazan, N. G. (2007) Omega-3 fatty acids, pro-inflammatory signaling and neuroprotection. *Curr. Opin. Clin. Nutr. Metab. Care 10*, 136−141.

(4) Nakanishi, H., Iida, Y., Shimizu, T., and Taguchi, R. (2010) Separation and quantification of sn-1 and sn-2 fatty acid positional isomers in phosphatidylcholine by RPLC-ESIMS/MS. *J. Biochem. 147*, 245−256.

(5) Dela, I., Popovic, M., Petrovic, T., Delas, F., and Ivanovic, D. (2008) Changes in the fatty acid composition of brain and liver phospholipids from rats fed fat-free diet. *Food Technol. Biotechnol. 46*, 278−285.

(6) Malhotra, A., Edelman-Novemsky, I., Xu, Y., Plesken, H., Ma, J., Schlame, M., and Ren, M. (2009) Role of calcium-independent phospholipase A2 in the pathogenesis of Barth syndrome. *Proc. Natl. Acad. Sci. U.S.A. 106*, 2337−2341.

(7) Beermann, C., Möbius, M., Winterling, N., Schmitt, J. J., and Boehm, G. (2005) sn-Position determination of phospholipid-linked fatty acids derived from erythrocytes by liquid chromatography electrospray ionization ion-trap mass spectrometry. *Lipids 40*, 211−218.

(8) Leitinger, N. (2003) Oxidized phospholipids as modulators of inflammation in atherosclerosis. *Curr. Opin. Lipidol. 14*, 421−430.

(9) Feldstein, A. E., Lopez, R., Tamimi, T. A., Yerian, L., Chung, Y. M., Berk, M., Zhang, R., McIntyre, T. M., and Hazen, S. L. (2010) Mass spectrometric profiling of oxidized lipid products in human nonalcoholic fatty liver disease and nonalcoholic steatohepatitis. *J. Lipid Res. 51*, 3046−3054.

(10) Adachi, J., Asano, M., Yoshioka, N., Nushida, H., and Ueno, Y. (2006) Analysis of phosphatidylcholine oxidation products in human plasma using quadrupole time-of-flight mass spectrometry. *Kobe J. Med. Sci. 52*, 127−140.

(11) Barroso, B., and Bischoff, R. (2005) LC-MS analysis of phospholipids and lysophospholipids in human bronchoalveolar lavage fluid. *J. Chromatogr., B: Anal. Technol. Biomed. Life Sci. 814*, 21−28.

(12) Huang, L. S., Kim, M. R., and Sok, D. E. (2009) Enzymatic reduction of polyunsaturated lysophosphatidylcholine hydroperoxides by glutathione peroxidase-1. *Eur. J. Lipid Sci. Technol. 111*, 584−592.

(13) Serhan, C. N., Chiang, N., and Van Dyke, T. E. (2008) Resolving inflammation: Dual anti-inflammatory and pro-resolution lipid mediators. *Nat. Rev. Immunol. 8*, 349−361.

(14) Jira, W., Spiteller, G., Carson, W., and Schramm, A. (1998) Strong increase in hydroxy fatty acids derived from linoleic acid in human low density lipoproteins of atherosclerotic patients. *Chem. Phys. Lipids 91*, 1−11.

(15) Vangaveti, V., Baune, B. T., and Kennedy, R. L. (2010) Hydroxyoctadecadienoic acids: Novel regulators of macrophage differentiation and atherogenesis. *Ther. Adv. Endocrinol. Metab. 1*, 51−60.

(16) Makidea, K., Kitamuraa, H., Satoa, Y., kutania, M., and Aoki, J. (2009) Emerging lysophospholipid mediators, lysophosphatidylserine, lysophosphatidylthreonine, lysophosphatidylethanolamine and lyso-phosphatidylglycerol. *Prostaglandins Other Lipid Mediators 89*, 135−139.

(17) Frasch, S. C., and Bratton, D. L. (2012) Emerging roles for lysophosphatidylserine in resolution of inflammation. *Prog. Lipid Res. 51*, 199−207.

(18) Croset, M., Brossard, N., Polette, A., and Lagarde, M. (2000) Characterization of plasma unsaturated lysophosphatidylcholines in human and rat. *Biochem. J. 345*, 61−67.

(19) Kagan, V. E., Shvedova, A. A., and Novikov, K. N. (1978) Participation of phospholipases in the "repair" of photoreceptor membranes subjected to peroxidation. *Biofizika 23*, 279−284.

(20) Van Kuijk, F. J., Sevanian, A., Handelman, G. J., and Dratz, E. A. (1987) A new role for phospholipase A2: Protection of membranes from lipid peroxidation damage. *Trends Biochem. Sci. 12*, 31−34.

(21) Salgo, M. G., Corongiu, F. P., and Sevanian, A. (1993) Enhanced interfacial catalysis and hydrolytic specificity of phospholipase A2 toward peroxidized phosphatidylcholine vesicles. *Arch. Biochem. Biophys. 304*, 123−132.

(22) Wilensky, L., Shi, Y., Mohler, I. E. R., Hamamdzic, D., Burgert, M. E., Li, J., Postle, A., Fenning, R. S., Bollinger, J. G., Hoffman, B. E., Pelchovitz, D. J., Yang, J., Mirabile, R. C., Webb, C. L., LeFeng Zhang, P., Gelb, M. H., Walker, M. C., Zalewski, A., and Macphee, C. H. (2008) Inhibition of lipoprotein-associated phospholipase A2 reduces complex coronary atherosclerotic plaque development. *Nat. Med. 14*, 1059−1066.

(23) Wilensky, R. L., and Macphee, C. H. (2009) Lipoprotein-associated phospholipase A(2) and atherosclerosis. *Curr. Opin. Lipidol. 20*, 415−420.

(24) Kriska, T., Marathe, G. K., Schmidt, J. C., McIntyre, T. M., and Girotti, A. W. (2007) Phospholipase action of platelet-activating factor acetylhydrolase, but not paraoxonase-1, on long fatty acyl chain phospholipid hydroperoxides. *J. Biol. Chem. 282*, 100−108.

(25) Fairn, G. D., Hermansson, M., Somerharju, P., and Grinstein, S. (2011) Phosphatidylserine is polarizied and required for proper Cdc42 localization and for development of cell polarity. *Nat. Cell Biol. 13*, 1424−1430.

(26) Kagan, V. E., Gleiss, B., Tyurina, Y. Y., Tyurin, V. A., Elenstrom-Magnusson, C., Liu, S.-X., Serinkan, F. B., Arroyo, A., Chandra, J., Orrenius, S., and Fadeel, B. (2002) A role for oxidative stress in apoptosis: Oxidation and externalization of phosphatidylserine is required for macrophage clearance of cells undergoing Fas-mediated apoptosis. *J. Immunol. 169*, 487−499.

(27) Kagan, V. E., Borisenko, G. G., Tyurina, Y. Y., Tyurin, V. A., Jiang, J., Potapovich, A. I., Kini, V., Amoscato, A. A., and Fujii, Y. (2004) Oxidative lipidomics of apoptosis: Redox catalytic interactions of cytochrome c with cardiolipin and phosphatidylserine. *Free Radical Biol. Med. 37*, 1963−1985.

(28) Kagan, V. E., Tyurin, V. A., Jiang, J., Tyurina, Y. Y., Ritov, V. B., Amoscato, A. A., Osipov, A. N., Belikova, N. A., Kapralov, A. A., Kini, V., Vlasova, I. I., Zhao, Q., Zou, M., Di, P., Svistunenko, D. A., Kurnikov, I. V., and Borisenko, G. G. (2005) Cytochrome c acts as a cardiolipin oxygenase required for release of proapoptotic factors. *Nat. Chem. Biol. 4*, 223−232.

(29) Tyurina, Y. Y., Kawai, K., Tyurin, V. A., Liu, S. X., Kagan, V. E., and Fabisiak, J. P. (2004) The plasma membrane is the site of selective phosphatidylserine oxidation during apoptosis: Role of cytochrome c. *Antioxid. Redox Signaling 6*, 209−225.

(30) Greenberg, M. E., Sun, M., Zhang, R., Febbraio, M., Silverstein, R., and Hazen, S. L. (2006) Oxidized phosphatidylserine-CD36 interactions play an essential role in macrophage-dependent phagocytosis of apoptotic cells. *J. Exp. Med. 203*, 2613−2625.

(31) Frasch, S. C., Berry, K. Z., Fernandez-Boyanapalli, R., Jin, H. S., Leslie, C., Henson, P. M., Murphy, R. C., and Bratton, D. L. (2008) NADPH oxidase-dependent generation of lysophosphatidylserine enhances clearance of activated and dying neutrophils via G2A. *J. Biol. Chem. 283*, 33736−33749.

(32) Fadeel, B., Xue, D., and Kagan, V. (2010) Programmed cell clearance: Molecular regulation of the elimination of apoptotic cell corpses and its role in the resolution of inflammation. *Biochem. Biophys. Res. Commun. 396*, 7−10.

(33) Ravichandran, K. S. (2011) Beginnings of a good apoptotic meal: The find-me and eat-me signaling pathways. *Immunity 35*, 445−455.

(34) Hosono, H., Aoki, J., Nagai, Y., Bandoh, K., Ishida, M., Taguchi, R., Arai, H., and Inoue, K. (2001) Phosphatidylserine-specific phospholipase A1 stimulates histamine release from rat peritoneal mast cells through production of 2-acyl-1-lysophosphatidylserine. *J. Biol. Chem. 276*, 29664−29670.

(35) Aoki, J., Nagai, Y., Hosono, H., Inoue, K., and Arai, H. (2002) Structure and function of phosphatidylserine-specific phospholipase A1. *Biochim. Biophys. Acta 1582*, 26−32.
(36) Tyurina, Y. Y., Serinkan, F. B., Tyurin, V. A., Kini, V., Yalowich, J. C., Schroit, A. J., Fadeel, B., and Kagan, V. E. (2004) Lipid antioxidant, etoposide, inhibits phosphatidylserine externalization and macrophage clearance of apoptotic cells by preventing phosphatidylserine oxidation. *J. Biol. Chem. 279*, 6056−6064.
(37) Tyurin, V. A., Tyurina, Y. Y., Feng, W., Mnuskin, A., Jiang, J., Tang, M., Zhang, X., Zhao, Q., Kochanek, P. M., Clark, R. S., Bayir, H., and Kagan, V. E. (2008) Mass-spectrometric characterization of phospholipids and their primary peroxidation products in rat cortical neurons during staurosporine-induced apoptosis. *J. Neurochem. 107*, 1614−1633.
(38) Folch, J., Lees, M., and Sloane Stanley, G. H. (1957) A simple method for the isolation and purification of total lipides from animal tissues. *J. Biol. Chem. 226*, 497−509.
(39) Malavolta, M., Bocci, F., Boselli, E., and Frega, N. G. (2004) Normal phase liquid chromatography-electrospray ionization tandem mass spectrometry analysis of phospholipid molecular species in blood mononuclear cells: Application to cystic fibrosis. *J. Chromatogr., B: Anal. Technol. Biomed. Life Sci. 810*, 173−186.
(40) Marvin Sketch was used for drawing, displaying the chemical structures, and generating the three-dimensional structures corresponding to the lowest-energy conformer: *Marvin*, version 5.3.6 (2010) ChemAxon (http://www.chemaxon.com).
(41) Samanta, U., Kirby, S. D., Srinivasan, P., Cerasoli, D. M., and Bahnson, B. J. (2009) Crystal structures of human group-VIIA phospholipase A2 inhibited by organophosphorus nerve agents exhibit non-aged complexes. *Biochem. Pharmacol. 78*, 420−429.
(42) Trott, O., and Olson, A. J. (2010) AutoDock Vina: Improving the speed and accuracy of docking with a new scoring function, efficient optimization, and multithreading. *J. Comput. Chem. 31*, 455−461.
(43) Sanner, M. F., Duncan, B. S., Carrillo, C. J., and Olson, A. J. (1999) Integrating computation and visualization for biomolecular analysis: An example using python and AVS. *Pac. Symp. Biocomput. '99*, 401−412.
(44) Lee, T., Malone, B., Longobardi, L., and Balestrieri, M. L. (2001) Differential regulation of three catalytic activities of platelet-activating factor (PAF)-dependent transacetylase. *Arch. Biochem. Biophys. 387*, 41−46.
(45) Davis, B., Koster, G., Douet, L. J., Scigelova, M., Woffendin, G., Ward, J. M., Smith, A., Humphries, J., Burnand, K. G., Macphee, C. H., and Postle, A. D. (2008) Electrospray ionization mass spectrometry identifies substrates and products of lipoprotein-associated phospholipase A2 in oxidized human low density lipoprotein. *J. Biol. Chem. 283*, 6428−6437.
(46) Gardner, A. A., Reichert, E. C., Topham, M. K., and Stafforini, D. M. (2008) Identification of a domain that mediates association of platelet-activating factor acetylhydrolase with high density lipoprotein. *J. Biol. Chem. 283*, 17099−17106.
(47) Stafforini, D. M., Tjoelker, L. W., McCormick, S. P., Vaitkus, D., McIntyre, T. M., Gray, P. W., Young, S. G., and Prescott, S. M. (1999) Molecular basis of the interaction between plasma platelet-activating factor acetylhydrolase and low density lipoprotein. *J. Biol. Chem. 274*, 7018−7024.
(48) McIntyre, T. M., Prescott, S. M., and Stafforini, D. M. (2009) The emerging roles of PAF acetylhydrolase. *J. Lipid Res. 50* (Suppl.), S255−S259.
(49) Chauffe, R. J., Wilensky, R. L., and Mohler, E. R., III (2010) Recent developments with lipoprotein-associated phospholipase A2 inhibitors. *Current Atherosclerosis Report 12*, 43−47.
(50) Magrioti, V., and Kokotos, G. (2010) Phospholipase A2 inhibitors as potential therapeutic agents for the treatment of inflammatory diseases. *Expert Opin. Ther. Pat. 20*, 1−18.
(51) Latchoumycandane, C., Marathe, G. K., Zhang, R., and McIntyre, T. M. (2012) Oxidatively truncated phospholipids are required agents of tumor necrosis factor α (TNFα)-induced apoptosis. *J. Biol. Chem. 287*, 17693−17705.
(52) Nakanishi, Y., Henson, P. M., and Shiratsuchi, A. (2009) Pattern recognition in phagocytic clearance of altered self. *Adv. Exp. Med. Biol. 653*, 129−138.
(53) Tyurina, Y. Y., Tyurin, V. A., Epperly, M. W., Greenberger, J. S., and Kagan, V. E. (2008) Oxidative lipidomics of γ-irradiation-induced intestinal injury. *Free Radical Biol. Med. 44*, 299−314.
(54) Tyurina, Y. Y., Tyurin, V. A., Kaynar, A. M., Kapralova, V. I., Wasserloos, K., Li, J., Mosher, M., Wright, L., Wipf, P., Watkins, S., Pitt, B. R., and Kagan, V. E. (2010) Oxidative lipidomics of hyperoxic acute lung injury: Mass spectrometric characterization of cardiolipin and phosphatidylserine peroxidation. *Am. J. Physiol. 299*, L73−L85.
(55) Obinata, H., and Izumi, T. (2009) G2A as a receptor for oxidized free fatty acids. *Prostaglandins Other Lipid Mediators 89*, 66−72.
(56) Kokotos, G., Hsu, Y. H., Burke, J. E., Baskakis, C., Kokotos, C. G., Magrioti, V., and Dennis, E. A. (2010) Potent and selective fluoroketone inhibitors of group VIA calcium-independent phospholipase A2. *J. Med. Chem. 53*, 3602−3610.
(57) Dennis, E. A., Cao, J., Hsu, Y. H., Magrioti, V., and Kokotos, G. (2011) Phospholipase A2 enzymes: Physical structure, biological function, disease implication, chemical inhibition, and therapeutic intervention. *Chem. Rev. 111*, 6130−6185.
(58) Min, J. H., Jain, M. K., Wilder, C., Paul, L., Apitz-Castro, R., Aspleaf, D. C., and Gelb, M. H. (1999) Membrane-bound plasma platelet activating factor acetylhydrolase acts on substrate in the aqueous phase. *Biochemistry 38*, 12935−12942.
(59) Cox, D., Fox, L., Tian, R., Bardet, W., Skaley, M., Mojsilovic, D., Gumperz, J., and Hildebrand, W. (2009) Determination of cellular lipids bound to human CD1d molecules. *PLoS One 4*, e5325.
(60) Freeman, G. J., Casasnovas, J. M., Umetsu, D. T., and DeKruyff, R. H. (2010) TIM genes: A family of cell surface phosphatidylserine receptors that regulate innate and adaptive immunity. *Immunol. Rev. 235*, 172−189.
(61) Kadl, A., Bochkov, V. N., Huber, J., and Leitinger, N. (2004) Apoptotic cells as sources for biologically active oxidized phospholipids. *Antioxid. Redox Signaling 6*, 311−320.
(62) Niki, E. (2009) Lipid peroxidation: Physiological levels and dual biological effects. *Free Radical Biol. Med. 47*, 469−484.
(63) Griendling, K. K., and FitzGerald, G. A. (2003) Oxidative stress and cardiovascular injury: Part II: Animal and human studies. *Circulation 108*, 2034−2040.
(64) Poulsen, H. E., Andersen, J. T., Keiding, N., Schramm, T. K., Sorensen, R., Gislasson, G., Fosbol, E. L., and Torp-Pedersen, C. (2009) Why epidemiological and clinical intervention studies often give different or diverging results? *IUBMB Life 61*, 391−393.
(65) Azzi, A. (2007) Oxidative stress: A dead end or a laboratory hypothesis? *Biochem. Biophys. Res. Commun. 362*, 230−232.
(66) Bazan, N. G. (2009) Cellular and molecular events mediated by docosahexaenoic acid-derived neuroprotectin D1 signaling in photoreceptor cell survival and brain protection. *Prostaglandins, Leukotrienes Essent. Fatty Acids 81*, 205−211.
(67) Gleissman, H., Yang, R., Martinod, K., Lindskog, M., Serhan, C. N., Johnsen, J. I., and Kogner, P. (2010) Docosahexaenoic acid metabolome in neural tumors: Identification of cytotoxic intermediates. *FASEB J. 24*, 906−915.
(68) DeLano, W. L. (2002) *The PyMOL User's Manual*, DeLano Scientific, Palo Alto, CA.